Student thesis series INES nr 544

Mapping Future Canadian Arctic Coastlines

Example of old coastlines under isostatic rebound conditions.
Bathurst Inlet, Nunavut (Beauregard 2013)

Pia Blake

2021
Department of
Physical Geography and Ecosystem Science
Lund University
Sölvegatan 12
S-223 62 Lund
Sweden

Pia Blake (2021).
Mapping Future Canadian Arctic Coastlines
Kartläggning av framtida arktiska kustlinjer i Kanada
Bachelor degree thesis, 15 credits in Physical Geography and Ecosystem Analysis
Department of Physical Geography and Ecosystem Science, Lund University

Level: Bachelor of Science (BSc)

Course duration: *January* 2021 until *June* 2021

Disclaimer

Mapping Future Canadian Arctic Coastlines

Pia Blake

Bachelor thesis, 15 credits, in Physical Geography and Ecosystem Analysis

Supervisor:
Marko Scholze
Lund University, Department of Physical Geography and Ecosystem Science

Exam committee:
Ulrik Mårtensson, Lund University
Petter Pilesjö, Lund University

Acknowledgements

Thanks to my supervisor, Marko Scholze, for guidance and feedback throughout this process. Thank you too to classmates for support and feedback, and to my family and friends for their encouragement and advice.

Abstract

The Canadian Arctic currently faces changing coastlines due isostatic rebound and climate change-driven sea-levels rising. This thesis seeks to answer how local coastlines will change over time under different Representative Concentration Pathway (RCP) scenarios, where errors in modelled coastlines come from, and how much of an impact isostatic rebound has on sea-levels compared to climate-change driven changes.

Maps which show changes in coastline through predicted sea-level changes in 2035, 2065, and 2100 have been produced through ArcGIS Pro's Forest-based regressions tool, with training data from historical climate variables and projection data under CMIP5 for RCP 2.6, 4.5, and 8.5, where RCP 2.6 refers to a low emissions scenario, RCP 4.5 refers to a moderate emissions scenario, and RCP 8.5 refers to a high emissions scenario. Isostatic rebound data can be sourced and run through the ICE-4G model. Multiple models were examined to ascertain which climate variables are needed to produce a stable model, using training data prior to and including 2000 and testing data post 2000 from 9 spatially diverse locations in the Canadian Arctic.

These results suggest that for Cambridge Bay, Resolute, and Alert, there will be little change in coastline under any RCP scenario. However, for Tuktoyaktuk coastlines are projected to advance significantly. While 9 locations total were used in during the process, only 4 were examined in greater detail due to data and time constraints. These finding should be considered when making plans for future coastal infrastructure.

Keywords: Isostatic Rebound, Canadian Arctic Climate Change, RCP scenarios, Coastlines

Table of Contents

1 Introduction 1

1.1 Study Aim 2

1.2 Hypotheses 2

2 Background and data sources 2

2.1 Isostatic Rebound 2

2.2 Mean Sea Level 3

2.3 RCP Scenarios 4

2.4 High Resolution DEM 4

2.5 Previous studies 4

3 Methodology 5

3.1 Study Site 5

3.2 Data processing 6

3.3 Sea level estimation 6

3.3.1 Mean Sea Level and Historical Climate Data 7

3.3.2 Isostatic Rebound Data 8

3.3.3 Future Climate Data 9

3.3.4 Forest-based Classification and Regression tool 9

3.4 DEMs 10

3.5 Combination of DEMs and Future predictions 10

4 Results 10

4.1 Isostatic Rebound 10

4.2 Model Analysis 11

4.3 Prediction using the model 14

4.4 Combined models 14

5 Discussion 23

5.1 Coastline map analysis 23

5.2 Model Validity 23

5.3 Limitations 24

5.4 Future Work 25
6 Conclusion 25
7 References 26
8 Appendix 29
8.1 Methodology 29
8.2 Isostatic Rebound 30
8.3 Sea Level change 30
8.4 Mean Sea Level 31
8.5 Regional climate 34
8.6 Additional Model Outputs 38
8.7 Future Climate Data 41

1 Introduction

Coastlines around the world are defined by the relationship between topography, bathymetry, and sea-level (Leverington et al. 2002). Baring large natural events, topography and bathymetry change on a geological timescale, while sea-level is mostly affected by climatic factors such as temperature and precipitation (Radic et al. 2014; Han et al. 2015). However, in the Canadian Arctic, the geologic factor of isostatic rebound also plays a measurable role in sea-level (Gough and Robinson 2000; Kaplan and Miller 2003; Han et al. 2015), making its inclusion in this thesis of vital importance.

Isostatic rebound is upward local adjustment of land once a glacier has retreated. The weight of the ice compresses the land during glaciation and rebound can take thousands of years on the scale of micro- or millimetres per year (Andrews 1968). In the case of the Canadian Arctic, glaciation ended around 8000 years ago, with rebound occurring today considered linear at a rate of a few millimetres per year – one of the fastest rates globally (Andrews 1968; Kaplan and Miller 2003; Tsuji et al. 2016).

Climatic factors affecting sea-level are more nuanced and change on a global to local level. Globally, land ice melt and sea surface temperature have the most impact on average sea-levels (Radic et al. 2014; Han et al. 2015), while local factors include those as well as wind patterns, local river inputs, tides, and the interaction of bathymetry with global oceanic circulation patters (Han et al. 2015; Johnson et al. 2019). At a global scale, sea-levels are rising due to climate change (Gough and Robinson 2000). Temperature is predicted to increase faster in the arctic compared to other regions of the world (Nkemdirim and Budikova 2001).

The combination of isostatic rebound and climatic factors have led to sea-levels falling in regions of the Canadian Arctic (Andrews 1968; Gough and Robinson 2000; Manson et al. 2005). Consequently, coastlines have been expanding onto newly emergent land (Tsuji et al. 2016) although the rate of emergence has slowed in some regions of the Canadian Arctic (Gough and Robinson 2000). While isostatic rebound can be assumed to be linear in time over 500 years (Leverington et al. 2002), climate change is affecting northern latitudes at a faster rate than the global average (Manson et al. 2005; Yu et al. 2020) leading to uncertainty of how coastlines will appear in future projections under different climate scenarios.

Coastlines have the greatest impact on Inuit, First Nations, Métis, and others living in the region, as hunting and fishing grounds are impacted (Johnson et al. 2019; Panikkar and Lemmond 2020) as well as treaty boundaries in regions of rapidly emergent land (Tsuji et al. 2016). Economically, shipping routes and other major infrastructure plans may be impacted by changing coastlines (van Luijk et al. 2020). This informs a need to project what coastlines may look like in future.

One recent study shows that climate change may result in reversal of the current sea-level falling in certain regions (Gough and Robinson 2000). Complex coastlines with small shallow bays and straits that characterise the Canadian Arctic coupled with small vertical changes in sea-level could result in dramatic local changes to coastlines (Johnson et al. 2019). Han et al. (2015) have mapped predicted sea-level changes on all Canadian coasts for RCP 8.5, although the focus was not on sea-level changes at coastlines but on changes for the region as a whole. There has also been work done to model coastlines directly post de-glaciation, using interpolation of data across the arctic against modern topography (Leverington et al. 2002). Both do emphasise, along with Manson et al. (2005), the challenges of interpolation across a large spatial region with few data points, and data series of which some are only a few decades old. Global sea level modelling has also taken place (Laboratory 2021), although as this is done at a global level it may differ from a model set on a local level.

1.1 Study Aim

The aim of this thesis is to predict Canadian Arctic coastlines at specific local areas for 2035, 2065, and 2100, given different IPCC RCP scenarios. This will be based on isostatic rebound data from Andrews (1968), climate data from Environment Canada and the Government of Canada, and sea level data from the Permanent Service for Mean Sea Level, part of the international organisation National Oceanography Centre (Holgate et al. 2012; PSMSL 2021).

1.2 Hypotheses

- Isostatic rebound will have a greater impact on sea-levels than climate-driven sea level change (Han et al. 2015).
- The prediction maps will have the greatest errors in the northern portion of the archipelago, where data is lacking spatially, and climate change will have a greater impact on climatic factors (Andrews 1968; Manson et al. 2005).
- Coastlines will be most emergent under lower Representative Concentration Pathways (RCP) scenarios and least under higher RCP scenarios (Gough and Robinson 2000; Han et al. 2015). RCP 2.6 is a low emissions scenario, with a global average warming of 0.9 to 2.3°C by 2090. RCP 4.5 is a moderate emissions scenario, with a global average warming of 1.7 to 3.2°C by 2090. RCP 8.5 is a high emissions scenario, with a global average warming of 3.2 to 5.4°C by 2090 (Canada 2021b).
- Changes to coastlines will be greatest along complex shallow coastlines due to there being more coastline to impact in a smaller region (Johnson et al. 2019).

2 Background and data sources

This section will introduce all the types and background to data used, the sources of the data and explain how each source of data is acquired and processed by the organisation responsible. This will be followed by a short section examining previous work done in this field of research.

2.1 Isostatic Rebound

Historically, isostatic rebound was measured by carbon dating organic material of found at ancient, uplifted coastlines (Andrews 1968; Forester et al. 1994; Petty et al. 1996). This, however, only shows regions where uplift has occurred and does not identify regions of subsistence. It also makes regions with a little uplift challenging to identify, as storms and high tides may remove evidence. For regions currently below sea level, such as off the coast of Nova Scotia, analysis of sea-floor sediments can give an indication of ancient coastlines (Forbes et al. 1991).

In Canada, isostatic rebound has been a part of indigenous knowledge since before contact, and was first written down in Hudson's Bay, Canada, as early as the early 1800's, prompted by observations that boats were unable to land at previously accessible harbours. At this time, the isostatic rebound at Churchill (a major city in Hudson's Bay) was estimated to be around 2.1 m/century (Wolf et al. 2006). More modern measurement location confirming this uplift can be seen in figure 1 at Churchill.

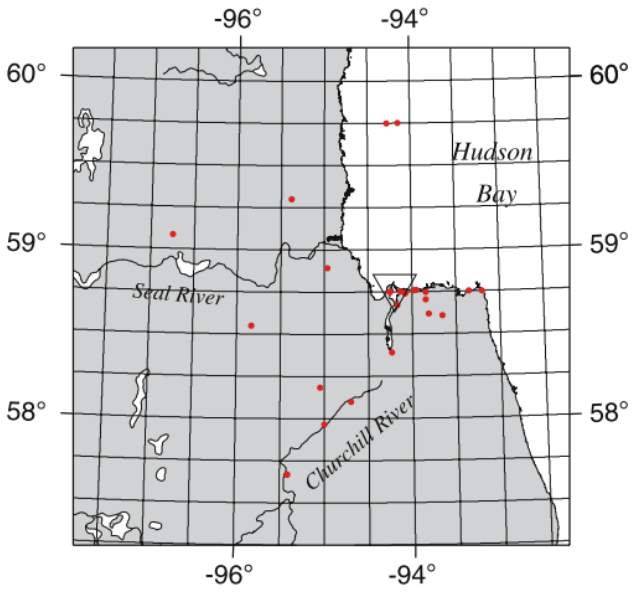

Figure 1: Map of Churchill region, showing location of carbon measurement in red, and a tide-gauge station in triangle. Location measurements used for isostatic rebound. Adapted from (Wolf et al. 2006).

As technology has advanced, methods of determining isostatic rebound have as well. Observations can now include movement of the mantle below surface, which helps to lift regions undergoing isostatic rebound. While the Canadian Arctic is seeing, in general, high rates of isostatic rebound, the emergent land is material which must come from somewhere else within the Earth's crust. This is the theory of compensation (Peltier 2004), which posits that the viscous nature of the mantle allows for ductile movement on the scale we observe in the Canadian Arctic. The theory of compensation allows for more precise models concerning isostatic rebound to be made.

In this thesis, isostatic rebound data will be taken from Andrews (1968) and Han et al. (2015), and run through the ICE-4G model (Peltier 2004).

2.2 Mean Sea Level

The Permanent Service for Mean Sea Level collects, publishes, analyses, and interprets sea level data from tide gauges around the world, and has since 1993 (Holgate et al. 2012; PSMSL 2021). Mean Sea Level (MSL) data is entered by the national authorities and measuring centres, and the data is then corrected to a common datum to obtain a revised local reference (RLR) (fig. 2). This correction is done using the tide gauge history at each location. The datum at each location is set to around 7000mm below mean sea level, to avoid negative numbers as sea levels fall relative to the previously established datum.

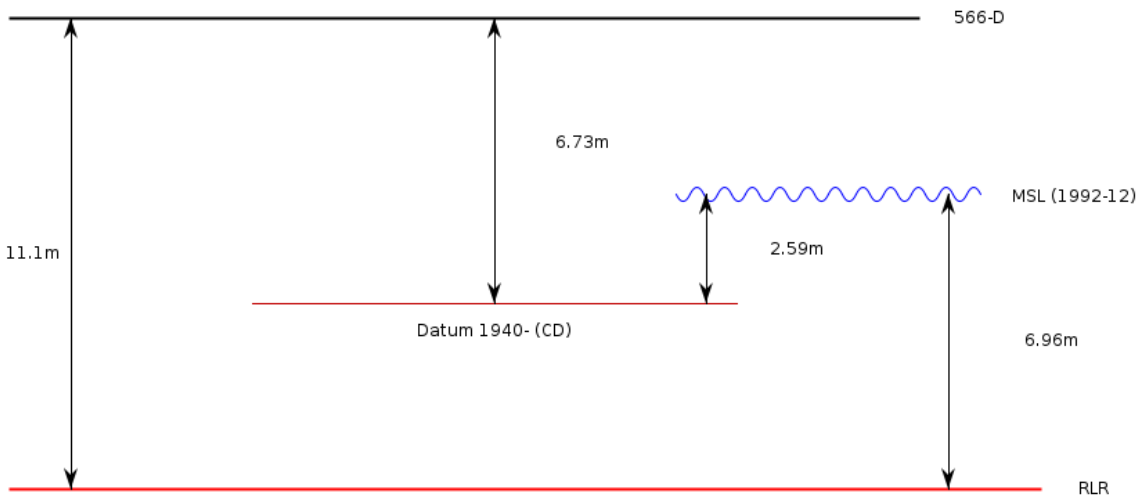

Figure 2: Adjustment of metric sea-level data at Churchill, Canada. MSL is the mean sea level, as measured. RLR is the relative sea-level, and acts as the datum from which MSL is recorded. Therefore, all values at Churchill are 6960mm higher than they were measured. Adapted from (Holgate et al. 2012; PSMSL 2021)

2.3 RCP Scenarios

RCP scenarios are used to represent potential future climate change scenarios based on differing emission scenarios. The future projections data for the thesis based on these 3 RCPs is based on the median (50th percentile) of the Coupled Model Intercomparison Project Phase 5 (CMIP5) (Canada 2021e; Laboratory 2021). This is a multi-model ensemble using 29 models, which are outline in Canada (2021e). Future projections in this model are based on a reference period of 1986-2005.

2.4 High Resolution DEM

The High Resolution Digital Elevation Model (HRDEM) for the Government of Canada is the source for topographic data used in this thesis. HRDEM is obtained from satellite imagery in northern Canada, and the current data sets available are derived from ArcticDEM, a public initiative from the National Geospatial-Intelligence Agency and the National Science Foundation to provide high resolution data in the Arctic (Canada 2021c). All elevation values have been set to the Canadian Geodetic Vertical Datum of 2013 (CGVD2013). HRDEM is available in 50 km by 50 km parcels, with each parcel having a unique grid location assigned to it. Vertical values are given to the nearest millimetre, and so an accuracy on the magnitude of a millimetre is assumed.

2.5 Previous studies

This thesis will be examining coastlines at a local scale for specific regions projected into the future. Studies which examine changing coastline projections on this scale were not found. However, there has been reconstruction of specific regions of Canadian Arctic coastlines up to the past Last Glacial Maximum (10 000 years ago) through addition of modern topography and projected isostatic rebound values (Leverington et al. 2002). This does not take climate change into account, but does provide a basis for how such a coastline projection paper can be approached.

In terms of isostatic rebound modelling, this thesis will use the model ICE-4G (Peltier 2004). This model, along with mean sea level data (Holgate et al. 2012; PSMSL 2021) has been used

in a previous study to obtain maps of relative sea level rise in Canadian waters (fig. 3) (Han et al. 2015). Note the lack of data in the Canadian Arctic.

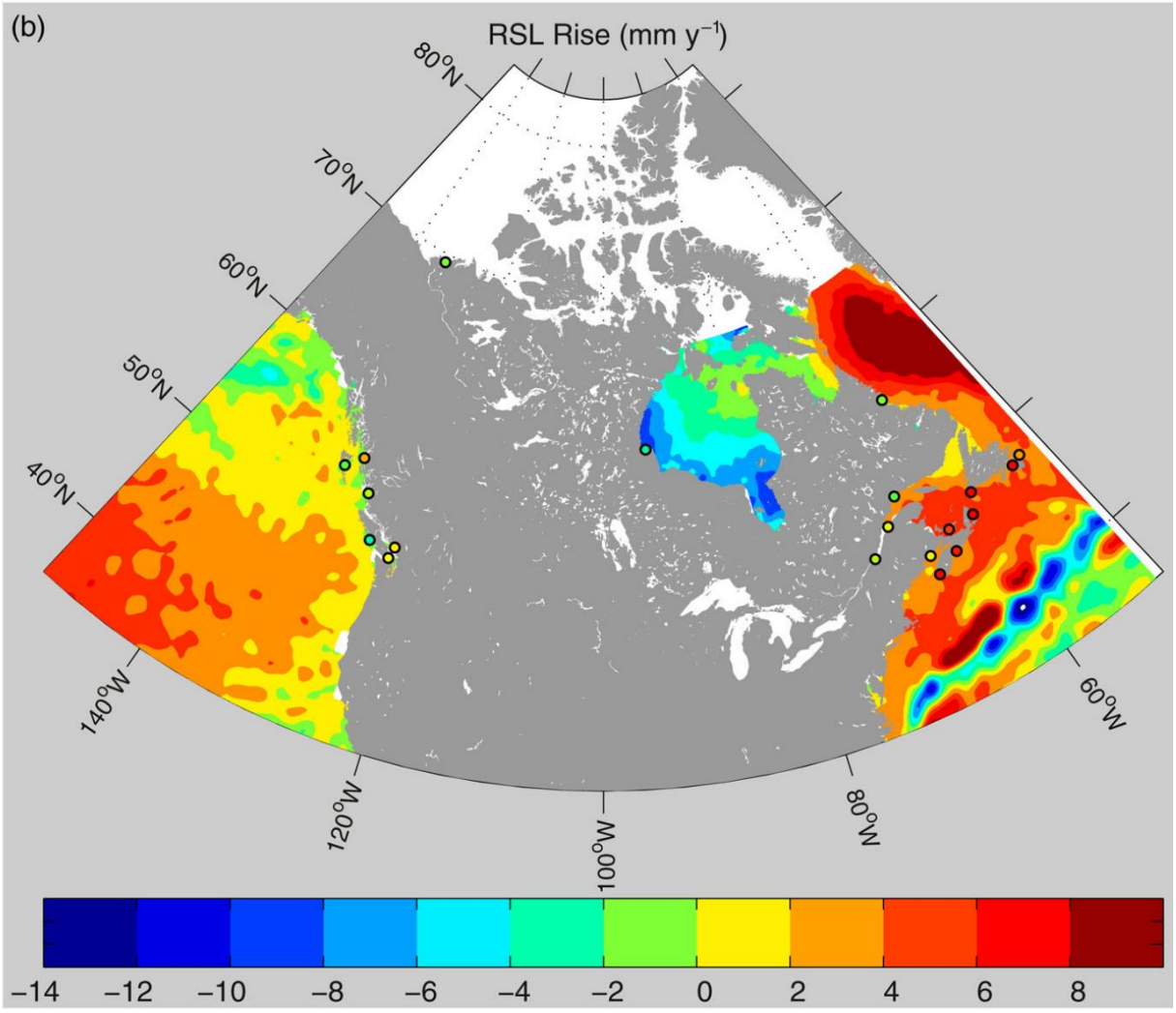

Figure 3:Relative Sea Level Rise based on RCP 8.5. Dots indicate locations where tide-gauge data was taken. Adapted from (Han et al. 2015).

On average, sea levels are rising at a rate of 10-20cm/century globally (Oerlemans et al. 2005). This estimated sea level rise is due to thermal expansion, glacial melt, but subject to regional uncertainty. However, we can see that this is not the case in the Canadian Arctic.

3 Methodology

3.1 Study Site

Projected coastlines were estimated for the Canadian Arctic Archipelago, which is in the northern hemisphere, forming a roughly cone-shaped region from roughly 53 degrees west to 135 degrees west, and extending from 55 degrees north northward (fig. 4). This region is classified as polar in the Köppen climate classification system (Volken et al. 2011), and the underlying geomorphology is shaped in large part by the recent glacial history of the region (Andrews 1968).

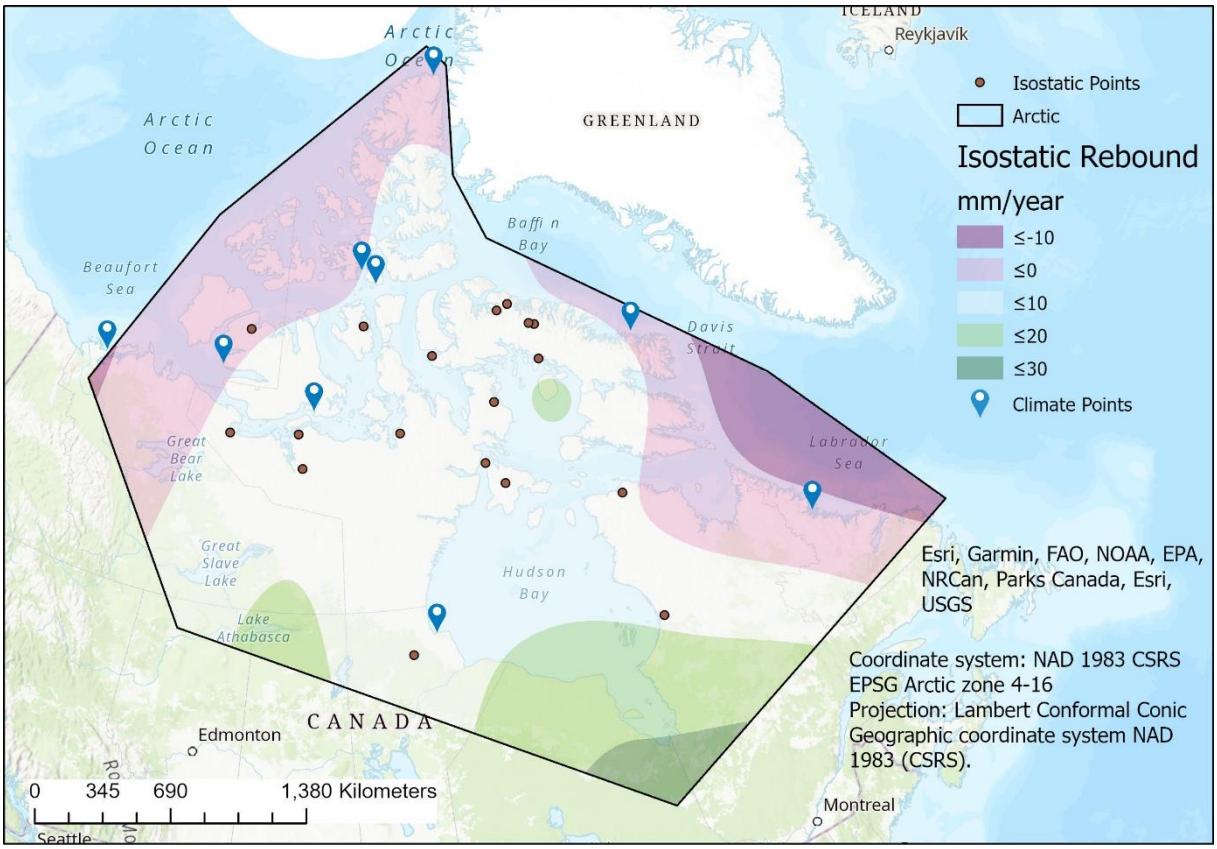

Figure 4: Isostatic rebound (mm/year) in the study area - roughly 53 degrees west to 135 degrees west, and extending from 55 degrees north northward, with isostatic points and climate measurement points identified.

The region is sparsely populated, which corresponds to few research and measurement stations, and those existing are scattered around the region. For this study, 9 measurement sites were chosen (Table 1) based on data availability. Data from these sites vary in length of data collection, as well as quality of data collection.

The climate of the region is diverse, with climate graphs for the data used in the final model shown in figures Appendix 11-Appendix 19.

3.2 Data processing

All data was clipped to the study area and projected into the coordinate system NAD 1983 CSRS EPSG Arctic zone 4-16, projection Lambert Conformal Conic, geographic coordinate system NAD 1983 (CSRS).

Processing of data was completed using Microsoft Excel 2010, and statistical evaluation of the results was completed through ArcGIS Pro and MatLab.

3.3 Sea level estimation

To project sea level based on differing climate scenarios, Mean Sea Level data, Historical Climate Data, Future Climate Data, and Isostatic Rebound Data were combined as outlined below using the Forest-based Classification and Regression tool in ArcGIS Pro.

3.3.1 Mean Sea Level and Historical Climate Data

Mean Sea Level data was sourced from the Permanent Service for Mean Sea Level (PSMSL 2021). Vertical values were given to the nearest millimetre, and so an accuracy on the magnitude of a millimetre was assumed. Data was found by searching through the list of available stations, ordered by latitude, and selecting those within Canadian waters which had been adjusted to the revised local reference (RLR). PSMSL data is available in monthly intervals, which informed later data selection. Initially, searching was restricted to those which had a continuous data set that covered most of the time frame 1951-2010 to cover two climate periods; however, this was revised as there was not sufficient data which completed that time frame. Nine stations were found which fit the Canadian waters and RLR criteria, a list of which is found in table 1 (Appendix 2 - Appendix 10).

Table 1: A summary of site locations, coordinates, and data sets' range and totals at that location. High Resolution Digital Elevation Model (HRDEM) grid location provided, if applicable.

Site	Coordinates	Date range	Number of data sets	HRDEM location
Resolute	74.691721 N, -94.809126 W	1957-1977	208	30_28
Cambridge Bay	69.091032 N, -105.097527 W	1965-1982	121	29_21
Tuktoyaktuk	69.466992 N, -132.975144 W	1961-1991, 2006	174	40_18
Churchill	58.768676 N, -94.239389 W	1947-2002	560	-
Alert	82.498974 N, -62.376189 W	1965-1977	98	33_38
Nain	56.54851 N, -61.698659 W	2001-2012	97	-
Little Cornwallis Island	75.388794 N, -96.930744 W	1992-1994	14	-
Ulukhaktok	70.736283 N, -117.76115 W	2003-2007	55	-
Qikiqtarjuaq	67.866667 N, -64.116667 W	2004-2006	24	-

Historical climate data was sourced from Environment Canada's Historical Data portal (Canada 2021a). Data was found by searching for station names which corresponded to those locations with mean sea level data. For each station, monthly data was selected as this corresponded to the time interval available for the mean sea level data. A summary of the variables and units can be found in table 2. Mean max temperature is the average of the daily

maximum temperature, mean minimum temperature of the average of the daily minimum temperature, mean temperature is the average temperature of the month, extreme max temperature is the maximum temperature recorded for that month, extreme min temperature is the minimum temperature recorded for that month, total rain is the total rainfall for the month, total snow is the total snowfall for the month, total precipitation is the total precipitation that fell in the month, and snow on ground last day is the amount of snow measured on the ground at the end of the month.

Table 2: A summary of data variables used, units, and sources.

Variable	Units	Source
Isostatic Rebound	mm/year	(Andrews 1968; Peltier 2004; Han et al. 2015)
Year	-	(Canada 2021a; PSMSL 2021)
Month	-	(Canada 2021a; PSMSL 2021)
Monthly Time-Gauge Data	mm	(Holgate et al. 2012; PSMSL 2021)
Mean Max Temperature	°C	(Canada 2021a)
Mean Min Temperature	°C	(Canada 2021a)
Mean Temperature	°C	(Canada 2021a)
Extreme Max Temperature	°C	(Canada 2021a)
Extreme Min Temperature	°C	(Canada 2021a)
Total Rain	mm	(Canada 2021a)
Total Snow	cm	(Canada 2021a)
Total Precipitation	mm	(Canada 2021a)
Snow on Ground, last day	cm	(Canada 2021a)
Climate Projections - CMIP5	-	(Canada 2021d, b)
Topography	m	(Canada 2021c)

Mean sea level data and the historical climate data was matched by month and year, missing data points were assigned a value of -99 999, and these data points were not considered for the forest-based classification because the regression tool is only able to work with completed data sets. A summary of the locations, date ranges, and number of final data sets can be found in table 1.

3.3.2 Isostatic Rebound Data

Isostatic rebound data point locations were sourced from Andrews (1968). This paper combined all previous isostatic rebound work in the Canadian Arctic into a total of 18 points. Spatially, spread was confined to the central portion of the study area, with lacking data points in the northern region of Ellesmere Island. Values in mm/year were calculated at each location using the formula from Peltier (2004), to give an isostatic rebound map as seen in figure 4. Interpolation to achieve the map was done in ArcGIS using the Spline method, with the spline type set to regularised and a weight of 0.1. Interpolation methods tried and tested by omission and testing from the surface created included Spline as well as Trend surfaces, Inverse Distance Weighting, and Kriging, with Spline having the highest final accuracy in predicting removed points.

Isostatic rebound rates in mm/year for each of the locations where historical climate data and mean sea level data was obtained were extracted from the interpolated surface, summarised in (Table Appendix 1). Isostatic rebound can be considered to be linear for a 500-year period, centered on the present day (Leverington et al. 2002). As such, the change in sea level attributable to isostatic rebound could be calculated by the formula:

$$Total\ isostatic\ rebound = (2021 - year) * Isostatic\ rebound\ rate$$

If the resulting value was negative, this indicated that the land was previously higher at that location compared to today, considering only isostatic rebound. If the resulting value was positive, this indicated that the land was previously lower at that location compared to today, considering only isostatic rebound.

Isostatic rebound for all RCP scenario and time frame projections were also calculated using the same formula, although there, if the resulting value was negative, this indicated that the land was projected to be higher at that location compared to today, considering only isostatic rebound. If the resulting value was positive, this indicated that the land was projected to be lower at that location compared to today, considering only isostatic rebound (Table Appendix 1).

3.3.3 Future Climate Data

Future Climate Data was sourced from the Government of Canada's global climate model scenarios portal (Canada 2021b). The data was downloaded as a region, with the interactive map zoomed out to the full extent of Canada.

Within the setting on the portal, the time interval was set to monthly, the value type was set to actual, and the ensemble percentile was set to the 50th percentile. As the historic climate data and mean sea level data was in monthly intervals, the future projections data also needed to be collected in monthly intervals. Due to time and computer storage restrictions, one month was chosen for all RCP scenarios and time frames. The month chosen for all maps was March, so the start and end dates were both set to March of the year in question. March was chosen as when examining the final historical data sets, this was the month with the most complete sets.

The variables downloaded were mean temperature (°C), mean daily precipitation (mm), and snow depth (m). Each variable was downloaded for a low emissions scenario (RCP 2.6), a moderate emissions scenario (RCP 4.5), and a high emissions scenario (RCP 8.5) for the years 2035, 2065, and 2100. These years were chosen as they are comparable to other sources found.

The regional maps were downloaded as GeoTIFFs and were projected into the correct coordinate system. They have a resolution of 1 degree.

Once in ArcGIS Pro, the values for each of the 27 rasters at the 9 locations were extracted, so that each location for each future year and each RCP scenario had a mean temperature (°C), mean daily precipitation (mm), and snow depth (m). Mean daily precipitation was converted into total precipitation for the month of March by multiplying the given value by 31, while snow depth was converted into cm. This was so that the future climate data variables match the input historical climate data.

3.3.4 Forest-based Classification and Regression tool

Forest-based regression was used to create a model that uses historical climate data, mean sea level data, and isostatic data to predict future sea levels. For this thesis, regression was used as the variables, both climatic and isostatic, are continuous. If the variables had been categorical, classification could have been used, or only certain variables could have been keyed as being categorical within the forest-based tool. All training variables were point features, hence no rasters were used as training data, testing data, or prediction data.

Forest-based regression is a supervised machine learning tool. It takes a subset of the training variables provided and creates decision trees which can then be used against a withheld validation dataset to test validity (Events 2019; 2.8 2021). For this thesis, 10% of training variables were left aside for validation of that particular model and the tool was set to run 100 random prediction trees. Both these parameters were the recommendations from Events (2019).

The model produced predicted values at each of the point features, which for this thesis are climate points in figure 4. The other outputs are a distribution of variable importance graph, and an output validation table. The distribution of variable importance graph helps to inform which variables are most important to the model. The output validation table provides the R^2 values for each of the random prediction trees run. This demonstrates the ability of the model to predict the training data which was excluded for validation. These two, along with parameter values (Table Appendix 3) can help to decide which variables to use in the final model.

Once variables which produced a statistically viable model, where the mean of the R^2 values was above 0.70 (Events 2019) was produced, the testing data was run against the future climate data to produce a value of predicted sea level change at each climate point. This value was in RLR and the units were mm, so to convert to m and true sea level change, the following formula was applied:

$$True\ sea\ level = (7000 - RLR\ sea\ level) * 1000$$

A summary of true sea levels can be found in table Appendix 2.

3.4 DEMs

Digital Elevation Model (DEM) data was sourced from the Government of Canada's High Resolution Digital Elevation Model's portal (Canada 2021c). The data was downloaded in 50km^2 sections at 2m resolution for the HRDEM locations in table 1.

Current coastlines were drawn from these 50km^2 sections using the extract tool, set to a range of -0.1m to +0.1m. This range gave a band to indicate modern day coastlines for each region (Leverington et al. 2002).

3.5 Combination of DEMs and Future predictions

The current coastline DEMs were examined to identify a region where a current coastline was clearly defined at a scale of 1:2000. The original DEM was then clipped to this location to limit disk space needed when creating each of the prediction DEMs. Each clipped DEM then had the change in sea level applied to all cells in the raster, and another extract tool set to a range of -0.1m to +0.1m gave the predicted coastline for that year and that RCP scenario.

An overview of the methodology can be found in figure Appendix 1.

4 Results

4.1 Isostatic Rebound

Isostatic rebound changes at each location are summarised in table Appendix 1. A visual representation can be seen in figure 4. Of note is the central rising isostatic rebound focussed on Hudson's Bay (Han et al. 2015). There are also regions where isostatic rebound is negative, surrounding these rising regions. For the climate points in figure 4, Churchill in the southern portion of the study area has the highest positive isostatic rebound rate and Tuktoyaktuk in the western portion of the study area has the highest negative isostatic rebound rate.

Figure 4 shows isostatic rebound up to 30mm/year south of James Bay. This is potentially a higher rate of isostatic rebound compared to other sources but is likely due to lacking data point in the southern region of the study area. This error may also be present at the northern most climate point: Alert, as there is little isostatic data available in this location.

4.2 Model Analysis

Initial test runs of the Forest-based regression model were run to predict sea level based on equal partitioning of the available climate and mean sea level data into two yearly time spans from 1951-1980 for training data and 1981-2010 for testing data. This excluded isostatic rebound data from the model and resulted in R^2 values with a mean lower than 0.40 based on ArcGIS's validation methods (fig. Appendix 20-Appendix 21).

Further investigation and discussion prompted the addition of isostatic rebound as a predicting variable, and the division of the data into training data being any data up to and including the year 2000, and testing data of the model to include all data post 2000. The new division of training and testing data was done to ensure more data sets in the training data for a more robust model.

First, the model was run using climate data from table 2, to get a sense of what the most important variables were (fig. 5). The variables used were the extreme temperature, the extreme minimum temperature, the snow on ground at the end of the month, the total precipitation in the month, the mean maximum temperature, the mean minimum temperature, and the mean temperature.

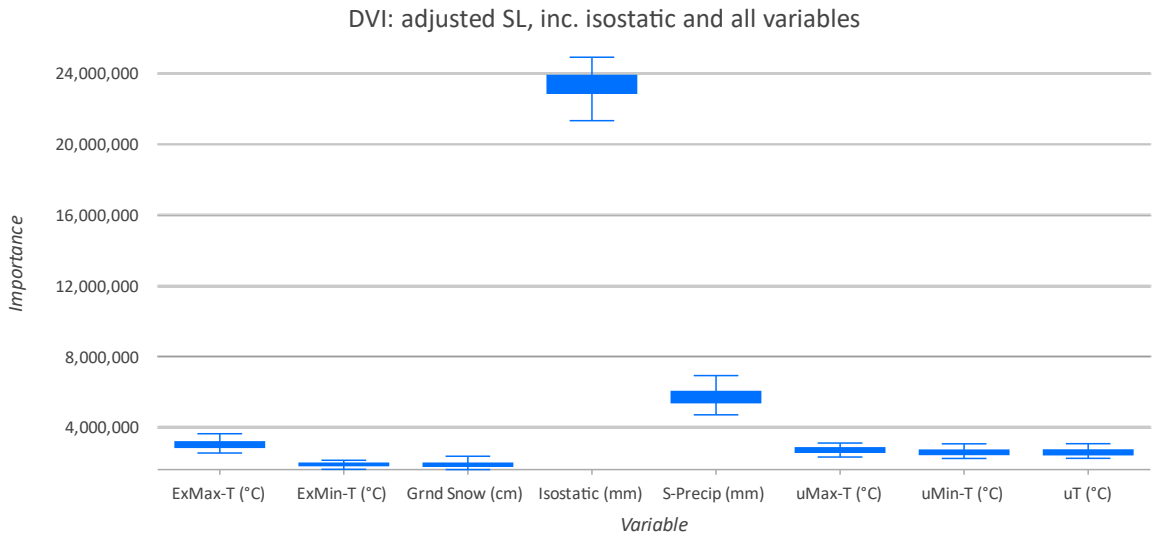

Figure 5: Distribution of Variable Importance graph for model run with adjusted sea level, including isostatic rebound, and all variables. ExMax-T is the extreme maximum temperature, ExMin-T is the extreme minimum temperature, Grnd Snow is the snow on the ground, Isostatic is the isostatic rebound, S-Precip is the total precipitation, uMax-T is the mean maximum temperature, uMin-T is the mean minimum temperature, and uT is the mean temperature.

Fig 5 shows that isostatic rebound is by far the most important variable in predicting sea level, with climatic variable ExMax-T and S-Precip being the most influential of those used.

The model was run 100 times, from which an output histogram can be created (fig. 6).

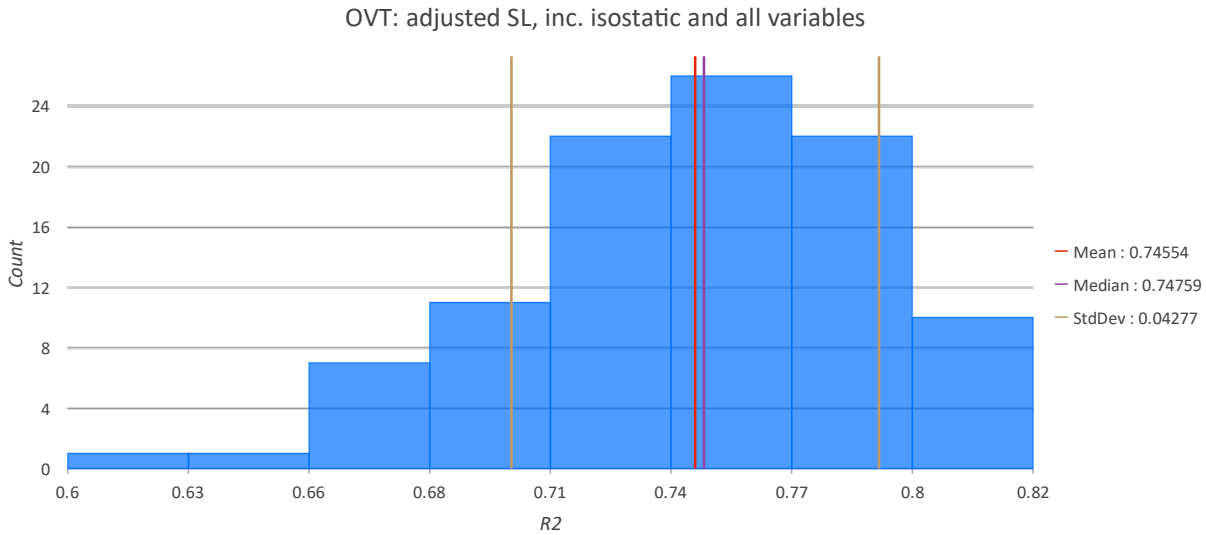

Figure 6: Output Validation Table, run on the variables from fig. 5 over 100 repetitions. This shows the R^2 values for each of the separate runs within a histogram.

This validation table shows that within ArcGIS's forest-based regression tool, the distribution of R^2 for each model has a mean of 0.75, which indicates a relatively stable model.

The model was run once more using those 3 as well as isostatic rebound. Figure 7 shows the distribution of variable importance and figure 8 shows the output validation table. The model was also run to predict the actual sea level (adjusted mean sea level-7000) instead of the adjusted mean sea level to see if there was a statistical difference (fig. Appendix 22 - Appendix 23). As none was found, all models moving forward use the adjusted mean sea level.

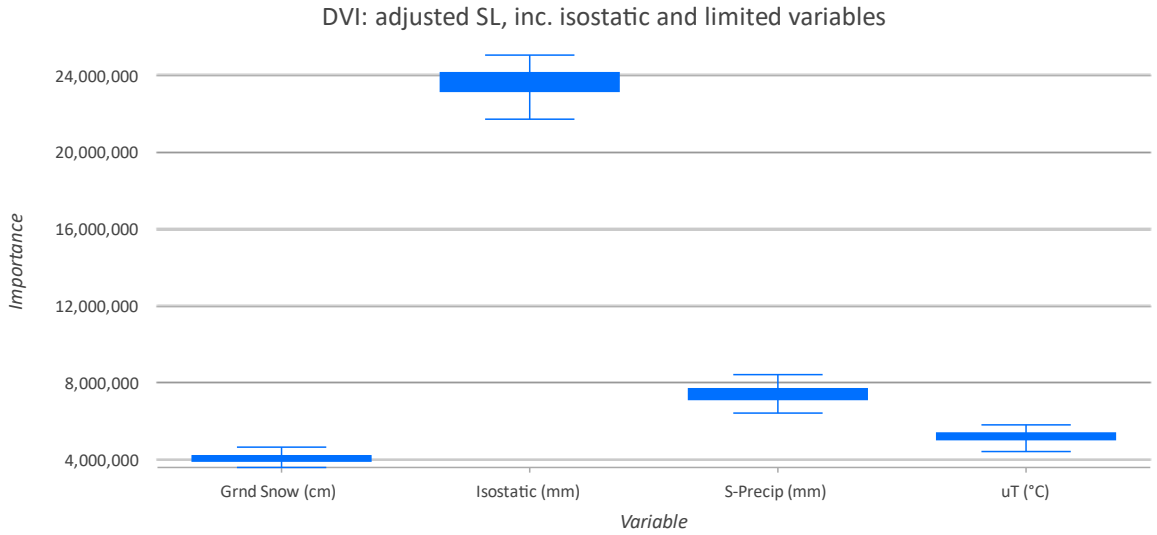

Figure 7: Distribution of Variable Importance graph for model run with adjusted sea level, including isostatic rebound, and limited variables. Grnd Snow is the snow on the ground, Isostatic is the isostatic rebound, S-Precip is the total precipitation, and uT is the mean temperature.

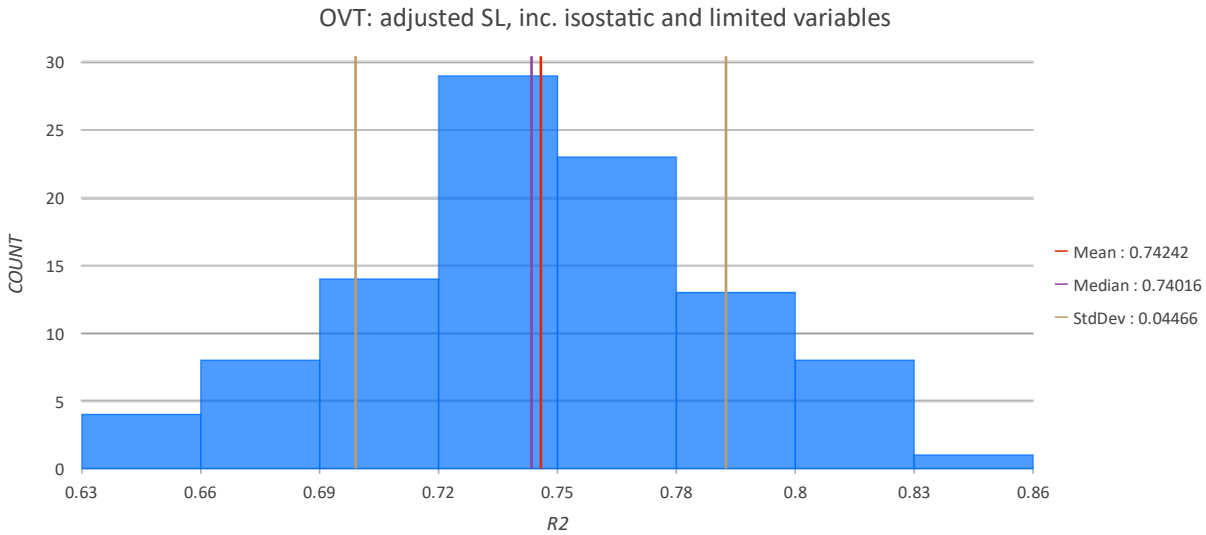

Figure 8: Output Validation Table, run on the variables from fig. 7 over 100 repetitions. This shows the R^2 values for each of the separate runs within a histogram.

Figure 7 shows that when run on limited variables, isostatic rebound is still the most important variable for predicting sea level. While the most important variables as identified in figure 5 were not all available for the future climate data, the validation table (fig. 8) shows that the distribution of R^2 for each model has a mean of 0.74, which indicates a relatively stable model comparable to the use of more climate variables. This is the final model used.

As sea level data exists for the testing data, and the above model gives predicted sea levels, these can be plotted against each other to test the ability of the model to predict sea levels. In figure 9, the measured sea level is plotted against the predicted sea level for all testing data sets. There is no relationship between the two, which suggests that the model did not do a good job of predicting sea levels. All geographical locations are used.

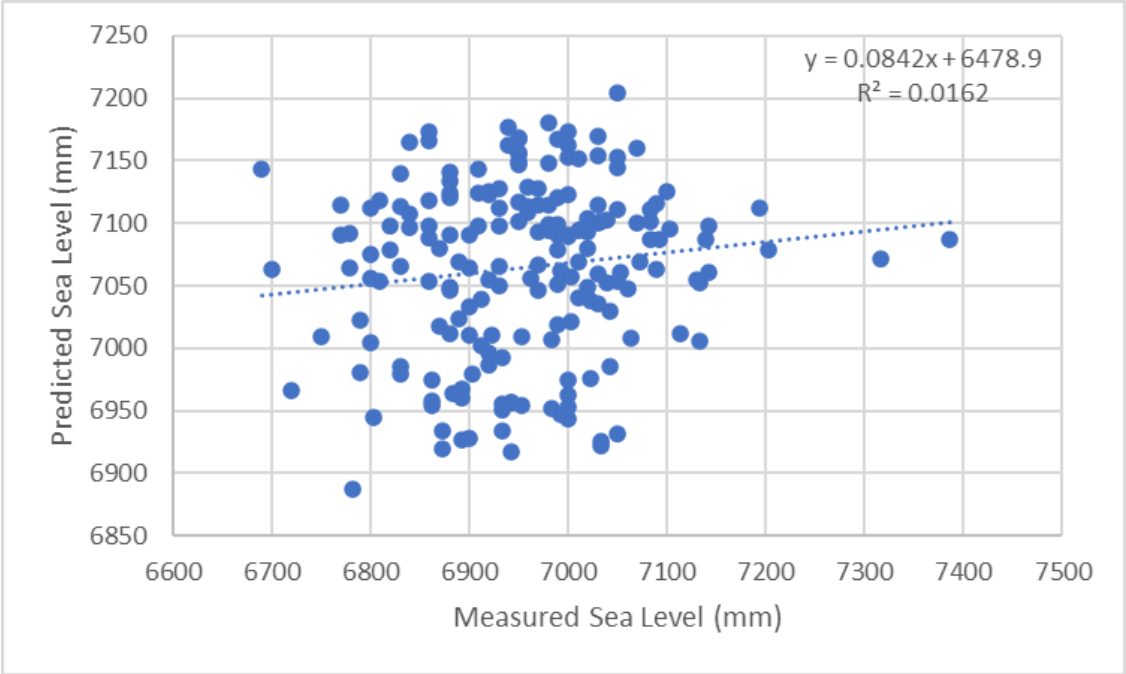

Figure 9: Measured sea level against predicted sea level for testing data based on the variables isostatic rebound, mean temperature, total precipitation, and snow on ground. Al geographical locations are used.

However, the testing data set includes data from locations where there are no data sets in the training data. These tend to be on the eastern portion of the study area. To investigate if the spatial scale of the data had an effect, figure 10 plots measured sea level against predicted sea level for only those locations in the western portion of the study area (Churchill, Tuktoyaktuk, Ulukhaktok). There is more of a relationship shown here, which is why the locations studied in more detail are in the western portion of the study area.

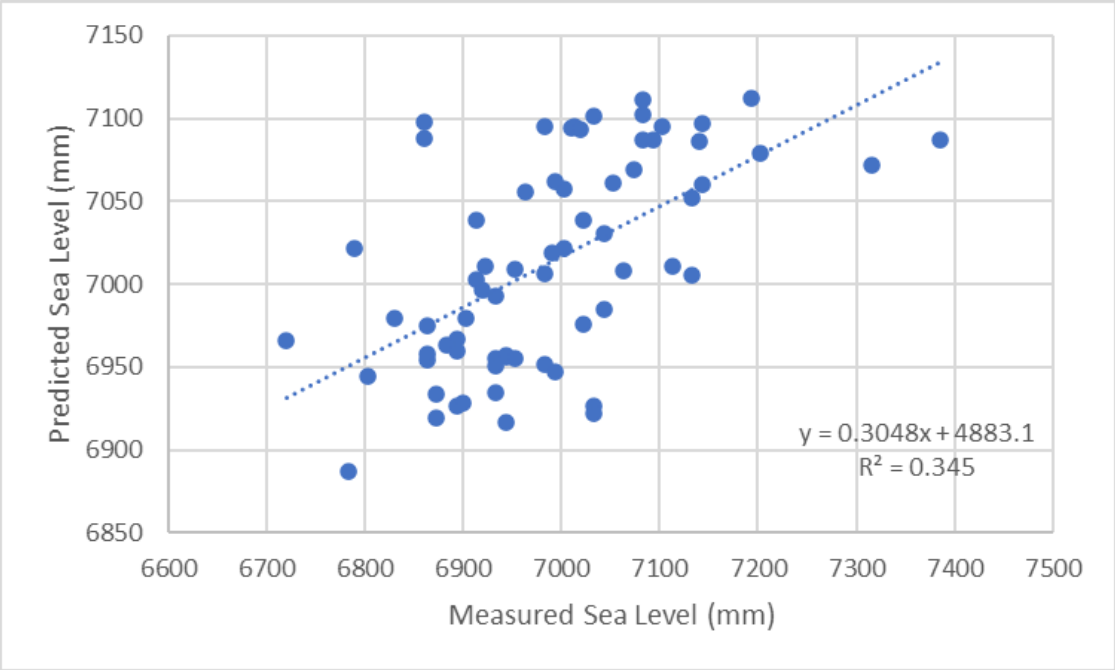

Figure 10: Measured sea level against predicted sea level for testing data based on the variables isostatic rebound, mean temperature, total precipitation, and snow on ground. Only including Churchill, Tuktoyaktuk, and Ulukhaktok.

4.3 Prediction using the model

The model was run using the training data, being any data up to and including the year 2000, and the 9 future scenarios, being a combination of the 3 RCP scenarios, and the 3 future years. This resulted in a value for sea predicted sea level at each climate location for each scenario.

The initial plan was to interpolate each of the 9 resulting scenarios across the region; however, this proved to result in larger files and processing need than the computers available were able to handle. As such, 4 locations in the study area (Tuktoyaktuk, Cambridge Bay, Resolute, and Alert) were chosen to produce future coastline maps. As there were DEMs available at each location, the predicted sea level rise was applied to each DEM as a single value, resulting in a vertical translation of each region of interest's DEM. The predicted sea level changes can be seen in table Appendix 2.

4.4 Combined models

For each of the 4 chosen locations the predicted coastlines can be visualised using the shifted DEMs and the predicted sea level changes from the Forest-based regression model, see figures 11-14. In all figures, the underlying blue and beige is from ArcGIS's underlying world map. It is not indicative of the current coastline but is used to show where land and water approximately are. As it can be challenging to see the change in the figures, the change in area from current coastlines is compiled in table 3. Figures Appendix 24 – Appendix 26 show future climate data compared to the changes in area from the current coastline.

Table 3:Change in area from the current coastline for each year and each RCP scenario. Positive values indicate coastline advance (land gained), and negative values indicate coastline retreat (land lost).

		Location			
Year	RCP scenario	Alert	Tuktoyaktuk	Resolute	Cambridge Bay
		Change in area from current coastline(m^2)			
2035	2.6	156	1728	-136	180
	4.5	1088	1604	904	124
	8.5	2376	1644	-96	20
2065	2.6	2364	-6480	220	72
	4.5	1456	-6580	860	268
	8.5	924	-6788	-80	144
2100	2.6	2840	-8268	1024	-320
	4.5	452	-8460	1076	324
	8.5	1648	-8408	1356	664

Figure 11 shows the change in coastlines at Alert. For each RCP scenario, black indicated the current coastline, green indicates projected coastline for 2035, blue indicates projected coastline for 2065, and red indicates projected coastline for 2100.

For RCP 2.6, some current coastline is visible, with a line of 2035 (green), little 2065 (blue), and the majority red (2100). This shows that the coastline is projected to advance slightly under RCP 2.6.

For RCP 4.5, some current coastline is visible, with no 2035 (green), little 2065 (blue), and the majority red (2100). Here, 2065 (blue) is observed beyond red (2100). This shows that the coastline is projected to advance to a maximum around 2065, and then retreat.

For RCP 8.5 some current coastline is visible, with a line of 2035 (green) beyond all other colours, a line of 2065 (blue) around the current coastline, and the majority red (2100). This shows that the coastline is projected to advance to a maximum around 2035, retreat to a minimum around the current coastline around 2065, and advance again to 2100. These changes are confirmed by table 3.

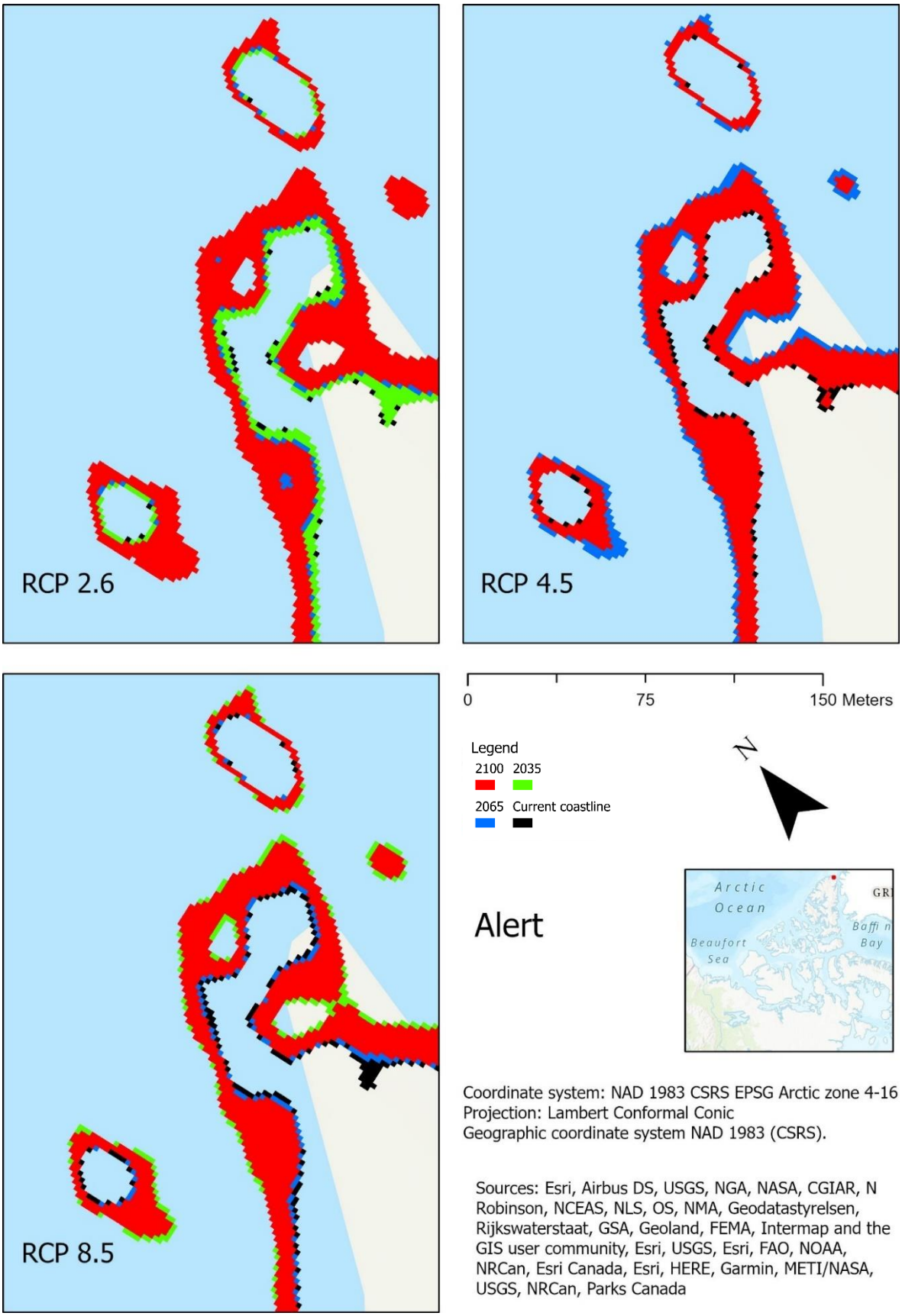

Figure 11 Predicted coastlines at Alert for RCP scenarios 2.6, 4.5, ad 8.5 for the years 2035, 2065, and 2100.

Figure 12 shows the change in coastlines at Cambridge Bay. For each RCP scenario, black indicated the current coastline, green indicates projected coastline for 2035, blue indicates projected coastline for 2065, and red indicates projected coastline for 2100.

For RCP 2.6, no current coastline is visible, with some 2035 (green), 2065 (blue), and the majority red (2100) moving towards the land. This shows that the coastline is projected to retreat slightly under RCP 2.6.

For RCP 4.5, very little other than 2100 (red) is visible This shows that the coastline is projected to remain where it is.

For RCP 8.5, very little other than 2100 (red) is visible This shows that the coastline is projected to remain where it is. These projections are confirmed by table 3, with changes in area of only a few hundred square meters.

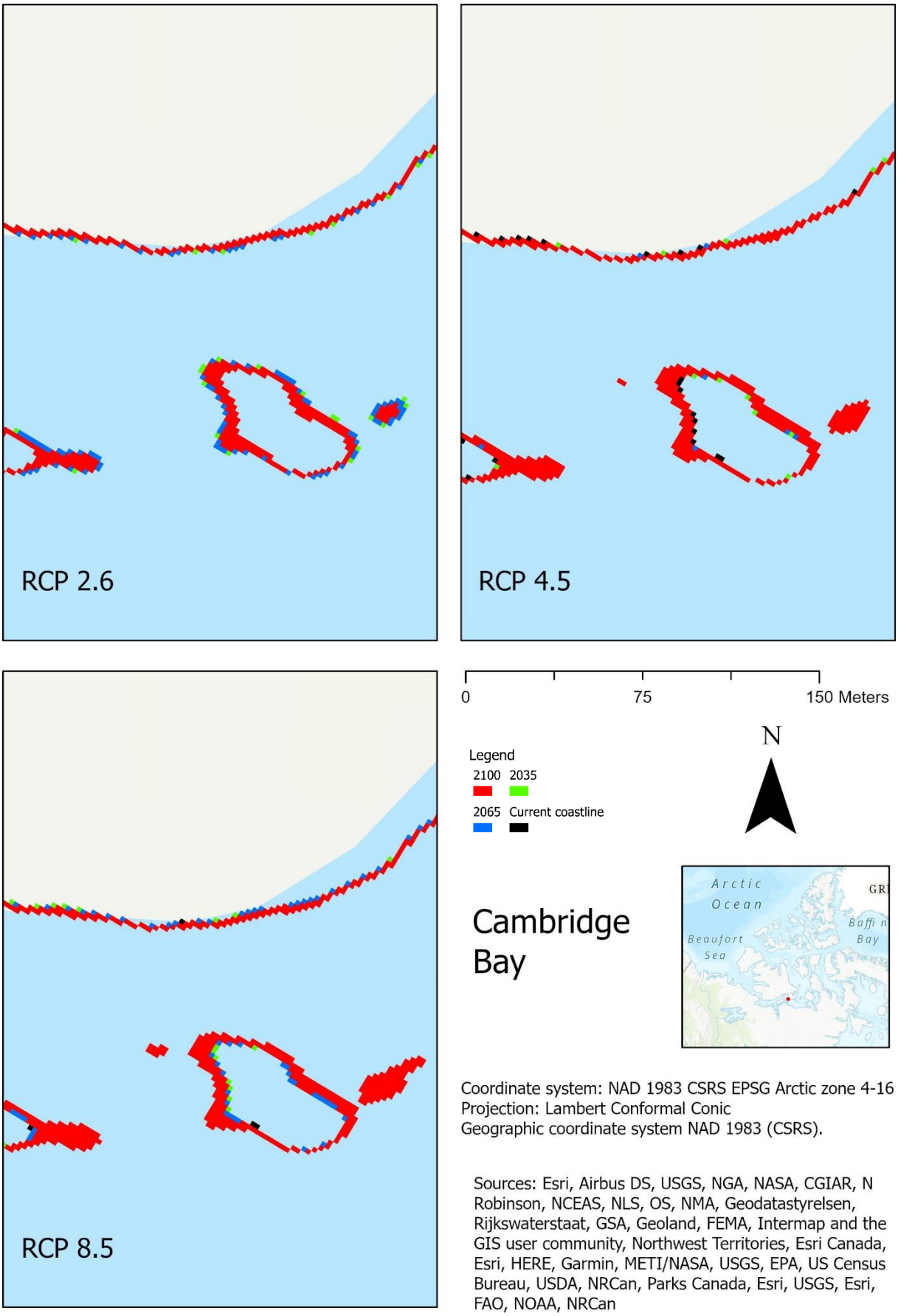

Figure 12: Predicted coastlines at Cambridge Bay for RCP scenarios 2.6, 4.5, ad 8.5 for the years 2035, 2065, and 2100.

Figure 13 shows the change in coastlines at Resolute. For each RCP scenario, black indicated the current coastline, green indicates projected coastline for 2035, blue indicates projected coastline for 2065, and red indicates projected coastline for 2100.

For RCP 2.6, no current coastline is visible, with some 2035 (green), 2065 (blue), and the majority red (2100) moving away from the land. This shows that the coastline is projected to advance slightly under RCP 2.6.

For RCP 4.5, some current coastline is visible, with no 2035 (green), little 2065 (blue), and the majority red (2100) moving away from the land. This shows that the coastline is projected to advance slightly under RCP 4.5, but that the advance occurs later than from RCP 2.6.

For RCP 8.5, no current coastline is visible, no 2035 (green), some 2065 (blue), and the majority red (2100) moving away from the land. This shows that the coastline is projected to advance under RCP 8.5 as well, but at an even later time than from RCP 4.5. These projections are confirmed by table 3.

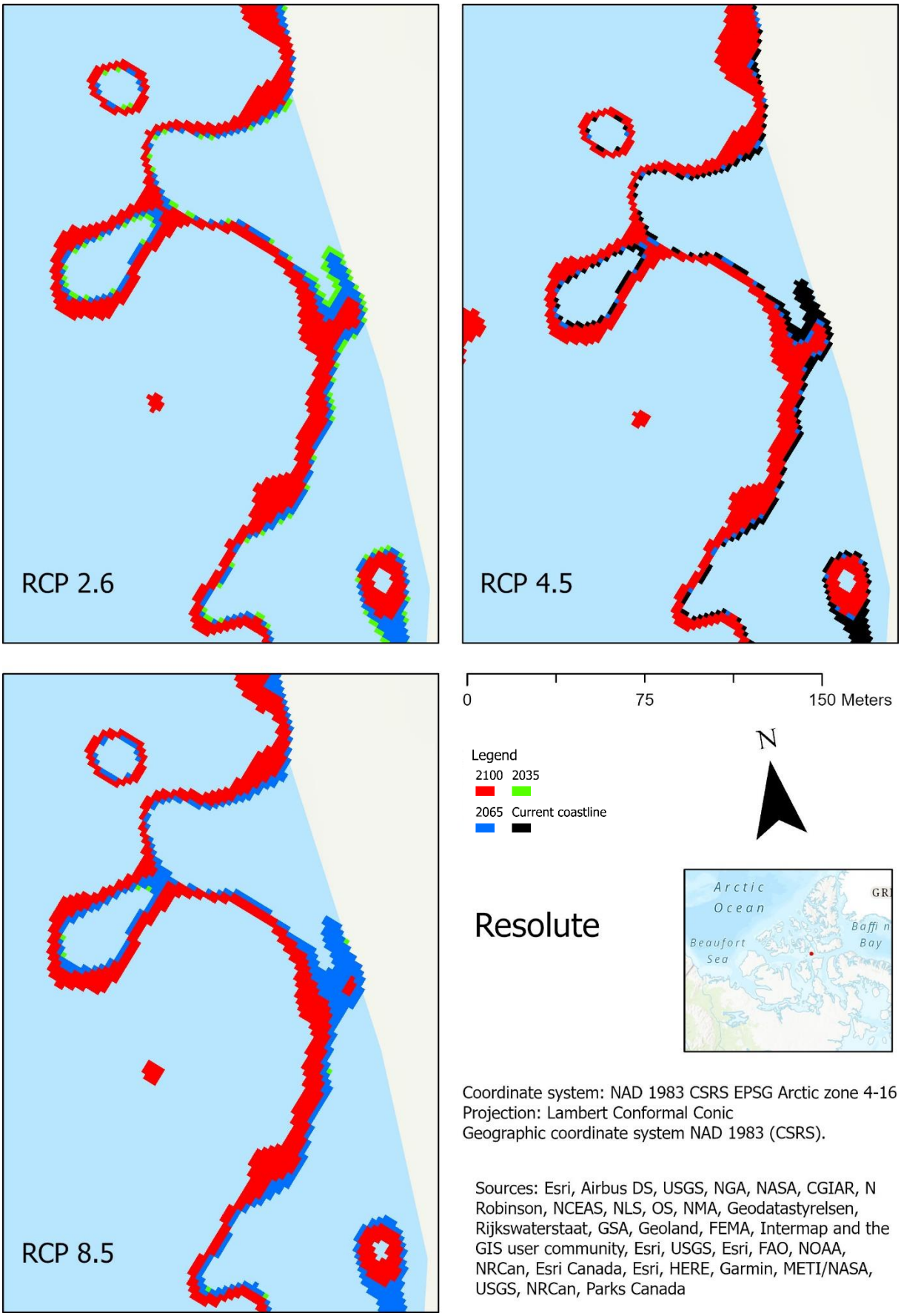

Figure 13: Predicted coastlines at Resolute for RCP scenarios 2.6, 4.5, ad 8.5 for the years 2035, 2065, and 2100.

Figure 14 shows the change in coastlines at Tuktoyaktuk. For each RCP scenario, black indicated the current coastline, green indicates projected coastline for 2035, blue indicates projected coastline for 2065, and red indicates projected coastline for 2100.

For RCP 2.6, current coastline is visible, 2035 (green) is visible towards sea from the current coastline, 2065 (blue) is visible towards land from the current coastline, and red (2100) is visible even more towards land from the current coastline. This shows that the coastline is projected to advance slightly to 2035, and then retreat to 2100 under RCP 2.6.

For RCP 4.5, current coastline is visible, 2035 (green) is visible towards sea from the current coastline, 2065 (blue) is visible towards land from the current coastline, and red (2100) is visible even more towards land from the current coastline. This shows that the coastline is projected to advance slightly to 2035, and then retreat to 2100 under RCP 4.5.

For RCP 8.5, current coastline is visible, 2035 (green) is visible towards sea from the current coastline, 2065 (blue) is visible towards land from the current coastline, and red (2100) is visible even more towards land from the current coastline. This shows that the coastline is projected to advance slightly to 2035, and then retreat to 2100 under RCP 8.5. There is very little variation between RCP scenarios. These projections are confirmed by table 3.

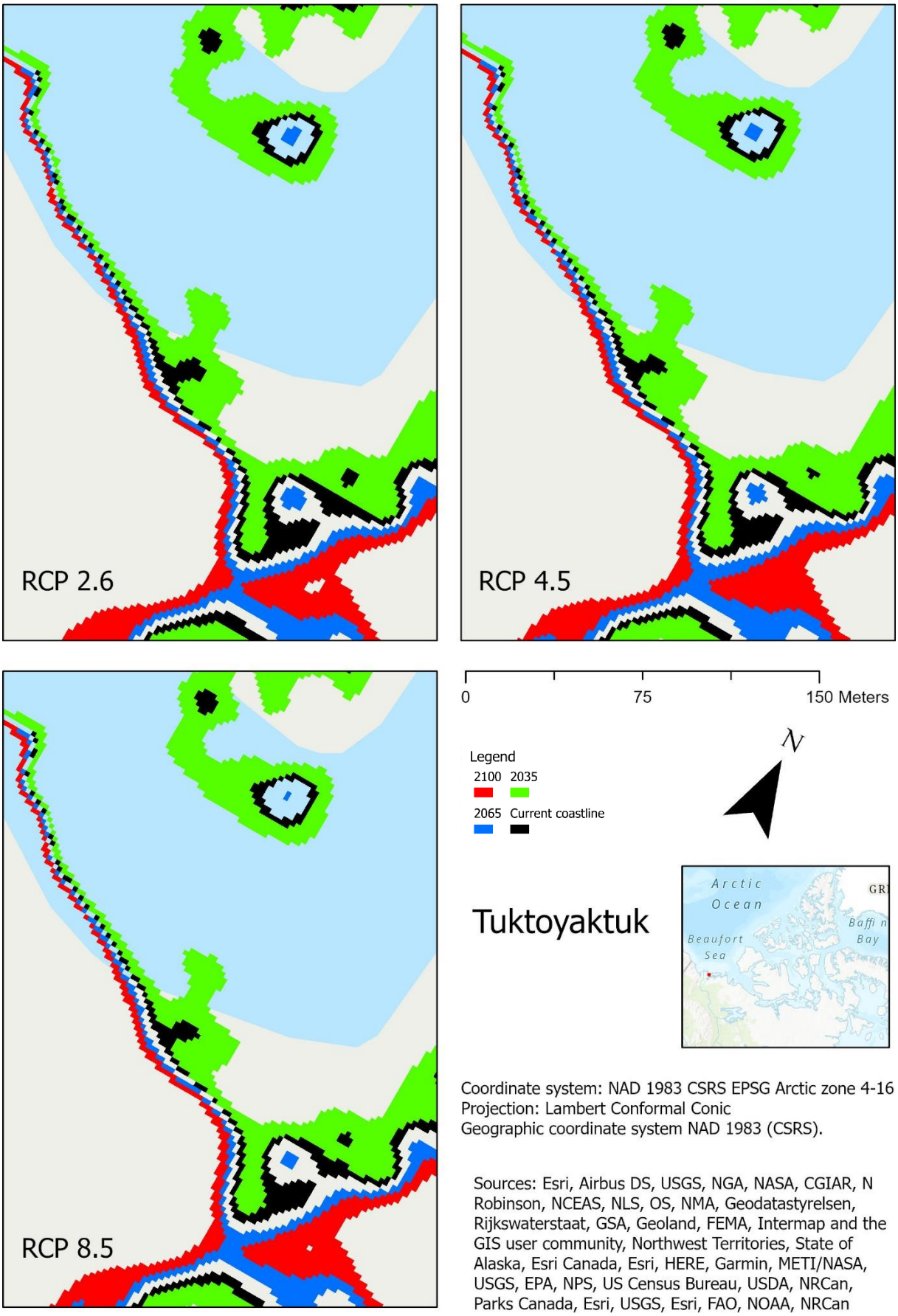

Figure 14: Predicted coastlines at Tuktoyaktuk for RCP scenarios 2.6, 4.5, ad 8.5 for the years 2035, 2065, and 2100.

5 Discussion

5.1 Coastline map analysis

Figures 11-14 show how coastlines could change at Alert, Tuktoyaktuk, Resolute, and Cambridge Bay over three RCP scenarios (2.6, 4.5, and 8.5) and for three different years (2035, 2065, and 2100).

At Alert, it appears that coastlines retreat under an RCP 2.6 scenario, are relatively stable under an RCP 4.5 scenario, and advance slightly under an RCP 8.5 scenario. This is in line with one of the hypotheses: Coastlines will be most emergent under RCP scenarios with lower projected temperature increase and least under RCP scenarios with higher projected temperature increase (Gough and Robinson 2000; Han et al. 2015). What is also visible here is that the range of coastline is quite large – around 75 horizontal meters. This suggests very gradual slopes to the underlying topography with the potential for large tidal ranges and the appearance and disappearance of small islands along the coast. This sloping coastal shelf could also contribute to a larger error in potential coastlines, as the overall space the coastline could occupy grows.

At Cambridge Bay, coastlines appear to be relatively consistent for all years at all RCP scenarios. There is slight potential growth of islands off the coast under RCP 8.5 due to shallow bays, but as this is on the scale of a few meters it is unlikely to be of much consequence.

At Resolute, a similar pattern to Alert is visible. However, unlike Alert it appears that there will be coastline retreat regardless of the RCP scenario, just that retreat is less under RCP 8.5 than under RCP 2.6 or 4.5.

At Tuktoyaktuk, a completely different pattern is visible. Here, regardless of the climate scenario, coastlines advance, creating new islands by cutting across shallow splits of land and obliterating other islands completely. Tuktoyaktuk is located on a thermokarst dominated low relief region (Manson et al. 2005), explaining part of this change, and a high rate of negative isostatic rebound contributes. Of all the regions studied, this shows the greatest modelled change in coastlines, which also corresponds to the hypothesis that changes to coastlines will be greatest along complex and shallow coastlines.

As there is little change at Tuktoyaktuk and Cambridge Bay under differing RCP scenarios, there is some indication that at these locations isostatic rebound has a greater impact on sea-levels than climate-driven sea level change.

While the changes observed are sometimes small on a local scale, these changes could amount to square kilometres of land being lost or gained in the Canadian Arctic, impacting coastal erosion, flooding, and migration patterns of animals (Vogel and Bullock 2020).

5.2 Model Validity

The isostatic rebound map (fig. 4) produced similar change patterns to other studies (Andrews 1968; Han et al. 2015). Isostatic rebound is centred on Hudson's Bay, with maxima rate there and a smaller one over Queen Maud Gulf. While current rates of isostatic rebound can be assumed to be correct, as isostatic rebound rates are multiplied across time to get a total change in vertical height due to isostatic rebound, any small errors incurred in the initial measurement are multiplied as well.

However, the isostatic map produced is also not identical to other maps created using the ICE-4G mode (Peltier 2004). In particular, the southern and northern portions of the study area differ. Values for isostatic rebound are greater negatively in the north and positively in the south in figure 4 compared to Peltier. This is likely due to few data points in those regions prior

to interpolation. In addition, the current method of some isostatic rebound measurement presumes that shorelines are perfect (Barletta and Bordoni 2013).

The final model used in this thesis is, according to ArcGIS's statistical analysis, sound. However, as seen in figure 9, when attempting to plot the known values of sea level against the predicted values of sea level little correlation is seen. This could be due to most of the training data for the model falling towards the western portion of the study area, while the testing data fell towards the eastern portion of the study area as divided by the times selected. A future run of the model may choose to divide the data differently to reduce this error source. Within this testing data set, 5 locations were represented (Churchill, Nain, Tuktoyaktuk, Ulukhaktok, and Qikiqtarjuaq). Of these 5, only 2 also had some data in the training data set (Churchill and Tuktoyaktuk). This is representative of a larger issue with the data available, which will be discussed in more detail below. As see in figure 10, the model is better at predicting sea levels in the western portion of the study area, leading to that region being used for deeper analysis.

The model analysis in figure 8 showed that similarly sound models could be obtained using only a few climate variables: in this case, mean temperature, monthly total precipitation, and snow cover. However, there are other variables which can be obtained in the same way from the Canadian government's climate scenarios (Canada 2021b). These include sea ice concentration, sea ice thickness, and ground wind-speed. It would have been interesting to investigate these further within the model, but historical climate data for the variables does not exist in sufficient quantities to derive a viable model using the Forest-based Classification and Regression tool.

An additional variable which has been the subject of local sea level papers is inputs from major rivers. At Churchill, there is a measurable influence from the local river on sea levels around its mouth (Gough and Robinson 2000). At a local level, this data may help to solidify the model used for creating coastline projections at a singular location. Additionally, the addition of previously landlocked water from melting glaciers into the arctic may contribute to local sea level rise, a factor which was not included here. Glaciers will contribute to a sea-level rise of 3.4±2.4cm over the next 100 years (Oerlemans et al. 2005), but this is assuming glaciers are currently in balance with the prevailing climate.

5.3 Limitations

The biggest limitation in this thesis is that of lacking data. As see in table 1, there are inconsistent spatial and temporal datasets, which likely contributed to a model that while sound by ArcGIS standards, does not stand up to other scrutiny. Other papers have noted this discrepancy too (Manson et al. 2005; Han et al. 2015) with some only looking at a small region where there is a longer series of data available – in this case Churchill (Wolf et al. 2006).

Another limitation encountered was that of processing power and storage space. This thesis was completed on a computer that is not entirely suited to run ArcGIS Pro and the files, in particular the DEMs, are quite large. As such, this thesis set out to model all coastlines across the study area but was unable to with the tools available.

The DEMs also limited where it was possible to observe coastline changes. In all regions where shallow bays were present, the application of the 'select by attributes' tool led to coastal flats being exposed. Coastal flats could be identified as regions where no discernible single coastline region was observed, but rather a block of raster cells falling within the select by attributes. Therefore, no change in coastline was easily observed.

Data quality and accuracy could also be classified as a limitation. The accuracy for the HRDEMs and tide gauge data was, based on the information available, assumed to be on the scale of millimetres in the vertical direction. If this data did not have an accuracy of millimetres but rather centimetres or metres, then the sea-level changes predicted could fall within the

centimetre or metre interval, and so no sea-level change could be observed. Consequently, there would be little to no change to the predicted coastlines for any of the locations.

5.4 Future Work

Creation of a model using the data available as open source at the moment may have been too ambitious, as there is not a long enough temporal range of data available nor is there a good spatial distribution over the Canadian Arctic. Investigation into other data sources would be advised, or scaling down of the investigation field to a local region would be a way around this limitation. On a short time scale, it is possible to observe how sea levels change purely based on tide gauge data (Koohzare et al. 2006).

The other variables mentioned above: sea ice concentration, sea ice thickness, and at ground wind-speed may help to improve the model, as well as consideration for inputs from local rivers and regional ice fields and glaciers.

Uncertainties could be calculated by running the same model using different projection percentiles for future climate data at each RCP scenario and year. For this thesis, there was a lack of time available.

Lastly, these exist sea-level projection data sets, to which the projected sea level from the model could be compared. Attempts were made to do this, but the data sets found covered the whole world, and due to lack of storage space and time, it was not possible to complete these comparisons.

6 Conclusion

The hypotheses were examined based on the 4 locations studied in greater detail within the larger study area. In conclusion:

- Isostatic rebound does have a greater impact on sea-levels than climate-driven sea level changes at Tuktoyaktuk and Cambridge Bay. This can be seen as there is little difference in coastline advance or retreat at these locations under differing RCP scenarios. At Resolute and Alert, there is variation in how and whether the coastlines advance or retreat under different RCP scenarios, indicating that climate-driven sea level changes have an impact at some locations and not at others.
- Alert is the northern-most location examined, and is the location where the most interesting advance and retreat cycles are observed. Under RCP 8.5, there is advance to 2035, retreat to 2065, and advance again for 2100. This could be indicative of the error on sea-levels increasing with northward movement where data is lacking spatially, and climate change having a greater impact on climatic factors.
- Coastlines were most emergent under RCP 2.6 scenarios at Alert and Tuktoyaktuk but were least emergent under RCP 2.6 scenarios at Cambridge Bay and Resolute. The opposite was true for RCP 8.5 scenarios.
- The most shallow and complex coastline region was Tuktoyaktuk, where coastline retreat was greatest and the most significant changes to coastline were observed.

7 References

2.8, A. P. 2021. How Forest-based Classification and Regression works. Retrieved, from https://pro.arcgis.com/en/pro-app/latest/tool-reference/spatial-statistics/how-forest-works.htm.

Andrews, J. T. 1968. Pattern and cause of variability of postglacial uplift and rate of uplift in Arctic Canada. *Journal of Geology,* 76**:** 404-425.

Barletta, V. R., and A. Bordoni. 2013. Effect of different implementations of the same ice history in GIA modeling. *Journal of Geodynamics,* 71**:** 65-73. DOI: 10.1016/j.jog.2013.07.002

Beauregard, M. 2013. Retrieved May 22 2021, from https://commons.wikimedia.org/wiki/File:Rebounding_beach,_among_other_things_(9404384095).jpg.

Canada, E. 2021a. Historical Climate Data. Retrieved April 9 2021, from https://climate.weather.gc.ca/index_e.html.

Canada, G. o. 2021b. Global climate model scenarios. Retrieved April 9 2021, from https://climate-change.canada.ca/climate-data/#/cmip5-data.

Canada, G. o. 2021c. High Resolution Digital Elevation Model (HRDEM) - CanElevation Series. Retrieved April 9 2021, from https://open.canada.ca/data/en/dataset/957782bf-847c-4644-a757-e383c0057995.

Canada, G. o. 2021d. Introduction to climate scenarios. Retrieved April 15, 2021 2021, from https://climate-scenarios.canada.ca/?page=cmip5-intro.

Canada, G. o. 2021e. Technical documentation: Coupled Model Intercomparison Project Phase 5 (CMIP5). Retrieved, from https://www.canada.ca/en/environment-climate-change/services/climate-change/canadian-centre-climate-services/display-download/technical-documentation-coupled-model-intercomparison-phase5.html.

Events, E. 2019. The Forest for the Trees: Making Predictions using Forest-Based Classification and Regression. Retrieved, from https://www.esri.com/videos/watch?videoid=kDAL2mKnae8&title=the-forest-for-the-trees-making-predictions-using-forest-based-classification-and-regression.

Forbes, D. L., R. Boyd, and J. Shaw. 1991. Late Quaternary Sedimentation and Se-Level Changes on the Inner Scotian Shelf. *Continental Shelf Research,* 11**:** 1155-1179. DOI: 10.1016/0278-4343(91)90095-n

Forester, R. M., S. M. Colman, R. L. Reynolds, and L. D. Keigwin. 1994. Lake Michigan's Late Quaternary Limnological and Climate History from Ostracode, Oxygen-Isotope, and Magnetic-Susceptibility. *Journal of Great Lakes Research,* 20**:** 93-107. DOI: 10.1016/s0380-1330(94)71134-5

Gough, W. A., and C. A. Robinson. 2000. Sea-level variation in Hudson Bay, Canada, from tide-gauge data. *Arctic, Antarctic, and Alpine Research,* 32**:** 331-335.

Han, G. Q., Z. M. Ma, N. Chen, R. Thomson, and A. Slangen. 2015. Changes in Mean Relative Sea Level around Canada in the Twentieth and Twenty-First Centuries. *Atmosphere-Ocean,* 53**:** 452-463. DOI: 10.1080/07055900.2015.1057100

Holgate, S. J., A. Matthews, P. L. Woodworth, L. J. Rickards, M. E. Tamisiea, E. Bradshaw, P. R. Foden, K. M. Gordon, et al. 2012. New Data Systems and Products at the Permanent Service for Mean Sea Level. *Journal of Coastal Research,* 29**:** 493-504. DOI: 10.2112/JCOASTRES-D-12-00175.1 %J Journal of Coastal Research

Johnson, A. C., J. Noel, D. P. Gregovich, L. E. Kruger, and B. Buma. 2019. Impacts of Submerging and Emerging Shorelines on Various Biota and Indigenous Alaskan Harvesting Patterns. *Journal of Coastal Research,* 35**:** 765-775. DOI: 10.2112/jcoastres-d-18-00119.1

Kaplan, M. R., and G. H. Miller. 2003. Early Holocene delevelling and deglaciation of the Cumberland Sound region, Baffin Island, Arctic Canada. *Geological Society of America Bulletin,* 115**:** 445-462. DOI: 10.1130/0016-7606(2003)115<0445:Ehdado>2.0.Co;2

Koohzare, A., P. Vanicek, and M. Santos. 2006. Compilation of a map of recent vertical crustal movements in Eastern Canada using geographic information system. *Journal of Surveying Engineering-Asce,* 132**:** 160-167. DOI: 10.1061/(asce)0733-9453(2006)132:4(160)

Laboratory, L. L. N. 2021. CMIP5 - Coupled Model Intercomparison Project Phase 5 - Overview. Retrieved April 7 2021, from https://pcmdi.llnl.gov/mips/cmip5/.

Leverington, D. W., J. T. Teller, and J. D. Mann. 2002. A GIS method for reconstruction of late Quaternary landscapes from isobase data and modern topography. *Computers & Geosciences,* 28**:** 631-639. DOI: 10.1016/s0098-3004(01)00097-8

Manson, G. K., S. M. Solomon, D. L. Forbes, D. E. Atkinson, and M. Craymer. 2005. Spatial variability of factors influencing coastal change in the western Canadian Arctic. *Geo-Marine Letters,* 25**:** 138-145. DOI: 10.1007/s00367-004-0195-9

Nkemdirim, L. C., and D. Budikova. 2001. Trends in sea level pressure across western Canada. *Journal of Geophysical Research-Atmospheres,* 106**:** 11801-11812. DOI: 10.1029/2001jd900060

Oerlemans, J., R. P. Bassford, W. Chapman, J. A. Dowdeswell, A. F. Glazovsky, J. O. Hagen, K. Melvold, M. D. de Wildt, et al. 2005. Estimating the contribution of Arctic glaciers to sea-level change in the next 100 years. In *Annals of Glaciology, Vol 42, 2005,* eds. J. Dowdeswell, and I. C. Willis, 230-236.

Panikkar, B., and B. Lemmond. 2020. Being on Land and Sea in Troubled Times: Climate Change and Food Sovereignty in Nunavut. *Land,* 9. DOI: 10.3390/land9120508

Peltier, W. R. 2004. GLOBAL GLACIAL ISOSTASY AND THE SURFACE OF THE ICE-AGE EARTH: The ICE-5G (VM2) Model and GRACE. *Annual Review of Earth & Planetary Sciences,* 32**:** 111-149. DOI: 10.1146/annurev.earth.32.082503.144359

Petty, W. H., P. A. Delcourt, and R. Hazel. 1996. Holocene lake-level fluctuations and beach-ridge development along the northern shore of Lake Michigan, USA. *Journal of Paleolimnology,* 15**:** 147-169.

PSMSL. 2021. Permanent Service for Mean Sea Level. Retrieved April 8 2021, from https://www.psmsl.org/.

Radic, V., A. Bliss, A. C. Beedlow, R. Hock, E. Miles, and J. G. Cogley. 2014. Regional and global projections of twenty-first century glacier mass changes in response to climate scenarios from global climate models. *Climate Dynamics,* 42**:** 37-58. DOI: 10.1007/s00382-013-1719-7

Tsuji, L. J. S., A. Daradich, N. Gomez, C. Hay, and J. X. Mitrovica. 2016. Sea level change in the western James Bay region of subarctic Ontario; emergent land and implications for Treaty No. 9. *Arctic,* 69**:** 99-107. DOI: 10.14430/arctic4542

van Luijk, N., J. Dawson, and A. Cook. 2020. Analysis of heavy fuel oil use by ships operating in Canadian Arctic waters from 2010 to 2018. *Facets,* 5**:** 304-327. DOI: 10.1139/facets-2019-0067

Vogel, B., and R. C. L. Bullock. 2020. Institutions, indigenous peoples, and climate change adaptation in the Canadian Arctic. *Geojournal*. DOI: 10.1007/s10708-020-10212-5

Volken, E., S. Brönnimann, and W. K̈oppen. 2011. The thermal zones of the Earth according to the duration of hot, moderate and cold periods and to the impact of heat on the organic world. *Meteorologische Zeitschrift,* 20**:** 351-360. DOI: 10.1127/0941-2948/2011/105

Wolf, D., V. Klemann, J. Wuensch, and F.-P. Zhang. 2006. A reanalysis and reinterpretation of geodetic and geological evidence of glacial-isostatic adjustment in the Churchill region, Hudson Bay. *Surveys in Geophysics,* 27**:** 19-61.

Yu, L. J., S. Y. Zhong, and B. Sun. 2020. Trends in the occurrence of pan-Arctic warm extremes in the past four decades. *International Journal of Climatology*. DOI: 10.1002/joc.7069

8 Appendix

8.1 Methodology

Figure Appendix 1: Methodology. Blue boxes are initial data, green boxes occur in excel, yellow boxes occur in ArcGIS Pro, orange boxes are analysis, and grey boxes are final results.

8.2 Isostatic Rebound

Table Appendix 1: Isostatic rebound at each climate point.

Site	Isostatic Rebound (mm/year)
Resolute	0.60
Cambridge Bay	4.19
Tuktoyaktuk	-10.30
Churchill	8.65
Alert	-2.67
Nain	-8.1
Little Cornwallis Island	-0.21
Ulukhaktok	-0.96
Qikiqtarjuaq	-2.72

8.3 Sea Level change

Table Appendix 2: Sea Level change under each scenario over time for the 4 locations chosen.

		Location			
		Resolute	Cambridge Bay	Tuktoyaktuk	Alert
Year	RCP Scenario	Sea Level change (m)			
2035	2.6	-0.006	0.020	0.085	0.005
	4.5	0.048	0.014	0.078	0.035
	8.5	-0.004	0.004	0.080	0.075
2065	2.6	0.012	0.010	-0.296	0.074
	4.5	0.046	0.026	-0.302	0.047
	8.5	-0.003	0.016	-0.316	0.029
2100	2.6	0.055	-0.030	-0.412	0.091
	4.5	0.057	0.030	-0.425	0.013
	8.5	0.073	0.057	-0.421	0.052

8.4 Mean Sea Level

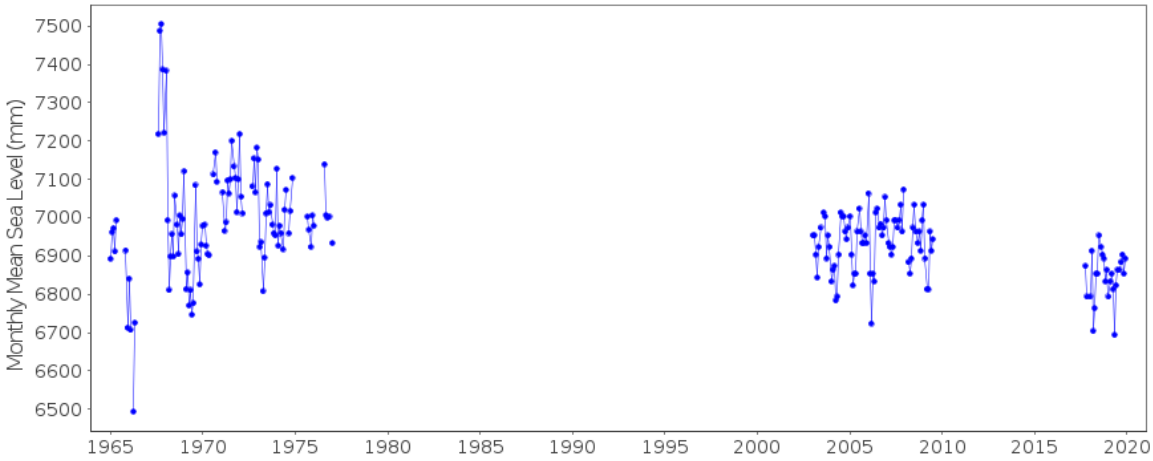

Figure Appendix 2: Mean Sea Level measurements: Alert (Holgate et al. 2012; PSMSL 2021)

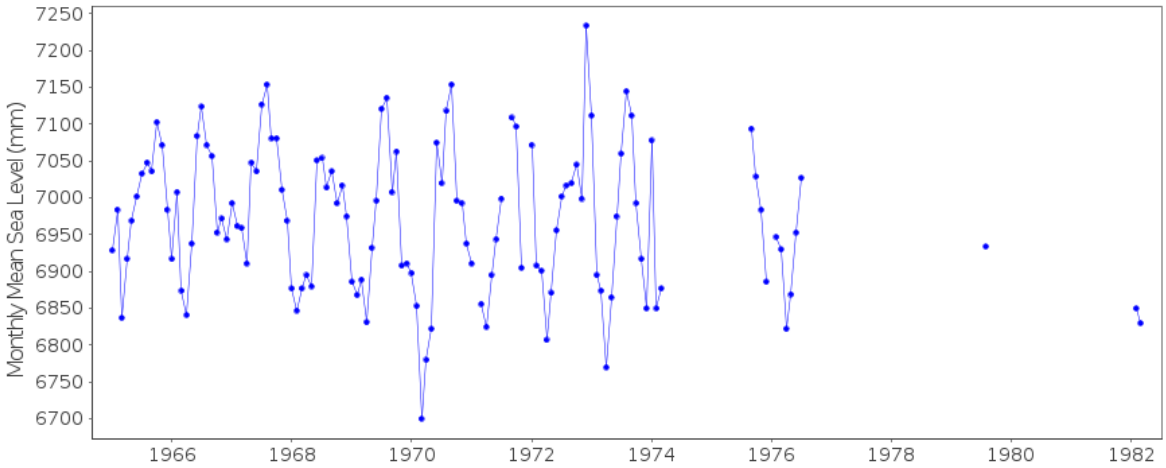

Figure Appendix 3: Mean Sea Level measurements: Cambridge Bay (Holgate et al. 2012; PSMSL 2021)

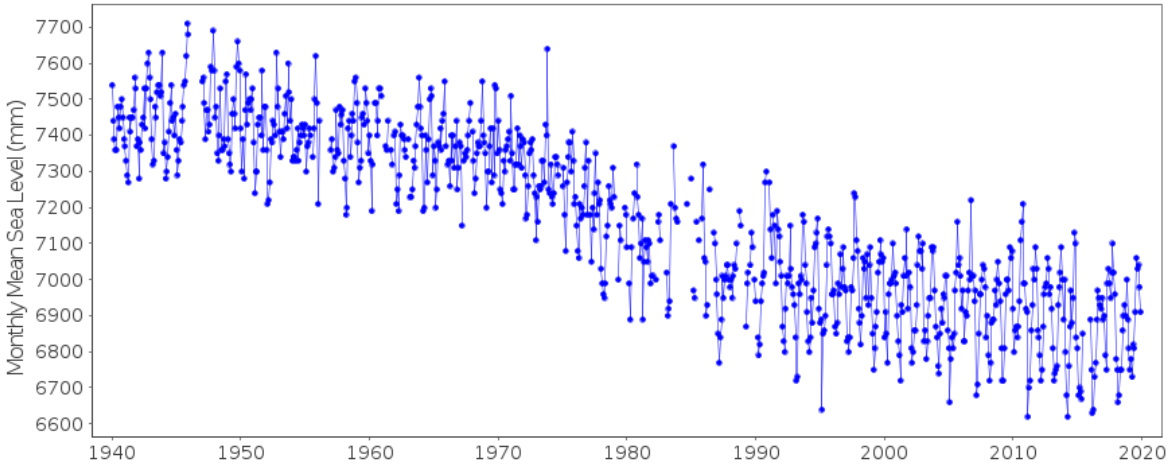

Figure Appendix 4: Mean Sea Level measurements: Churchill (Holgate et al. 2012; PSMSL 2021)

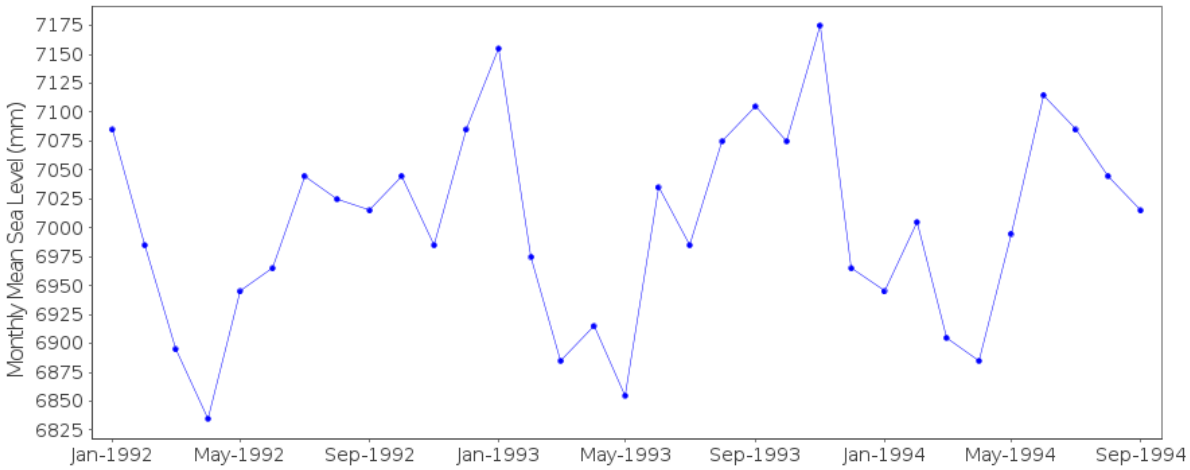

Figure Appendix 5: Mean Sea Level measurements: Little Cornwallis Island (Holgate et al. 2012; PSMSL 2021)

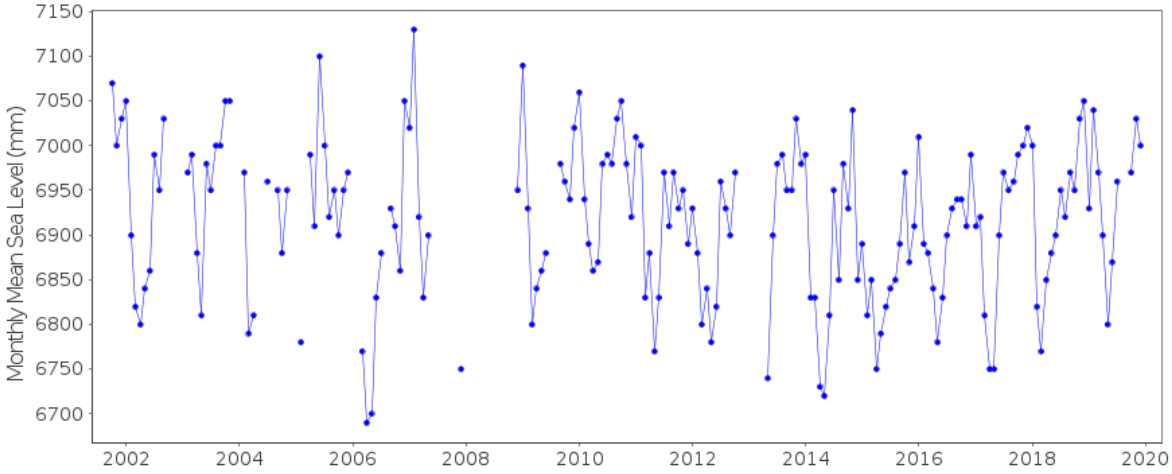

Figure Appendix 6: Mean Sea Level measurements: Nain (Holgate et al. 2012; PSMSL 2021)

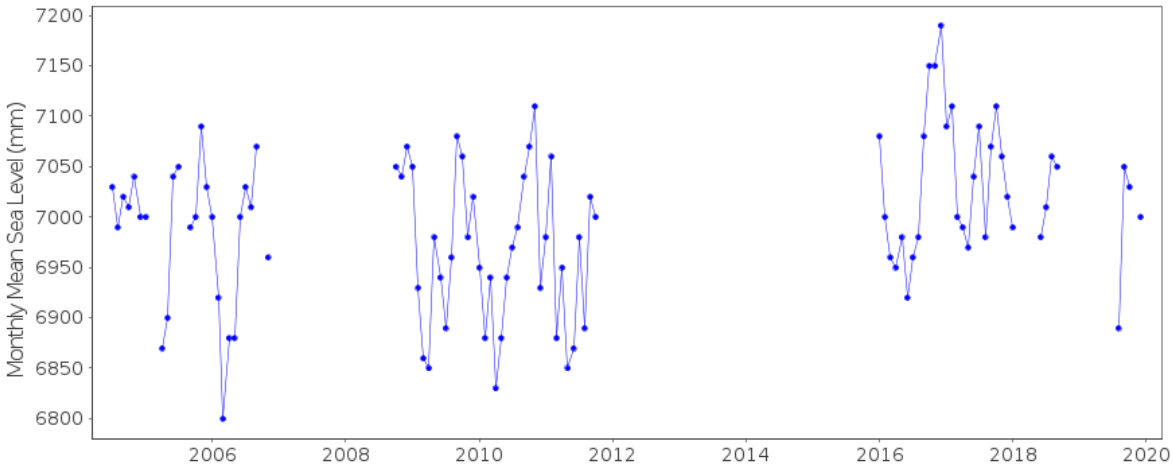

Figure Appendix 7: Mean Sea Level measurements: Qikiqtarjuaq (Holgate et al. 2012; PSMSL 2021)

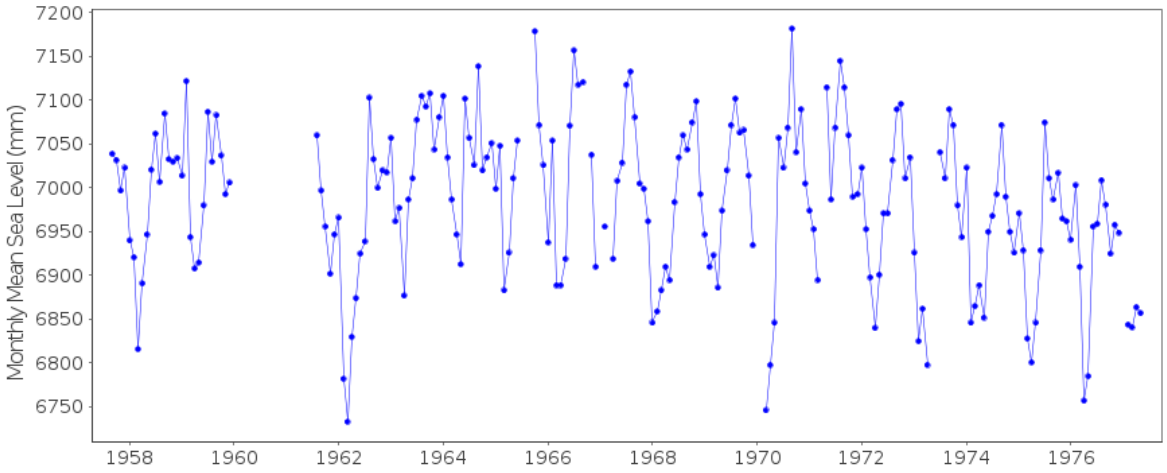

Figure Appendix 8: Mean Sea Level measurements: Resolute (Holgate et al. 2012; PSMSL 2021)

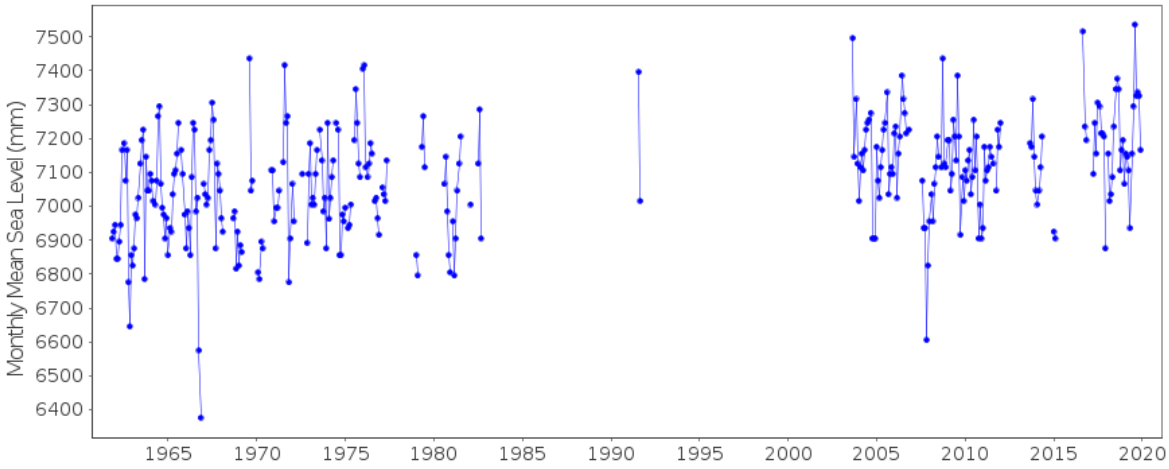

Figure Appendix 9: Mean Sea Level measurements: Tuktoyaktuk (Holgate et al. 2012; PSMSL 2021)

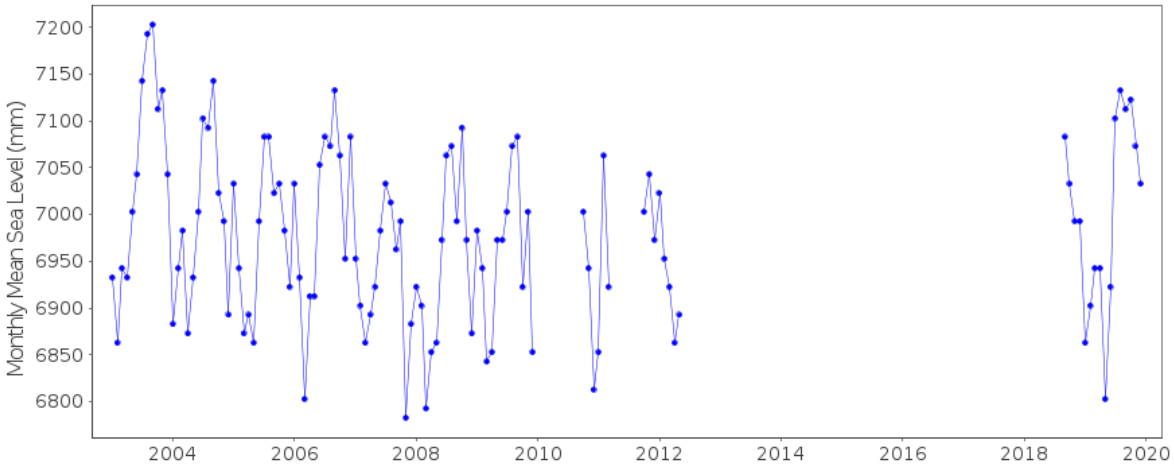

Figure Appendix 10: Mean Sea Level measurements: Ulukhaktok (Holgate et al. 2012; PSMSL 2021)

8.5 Regional climate

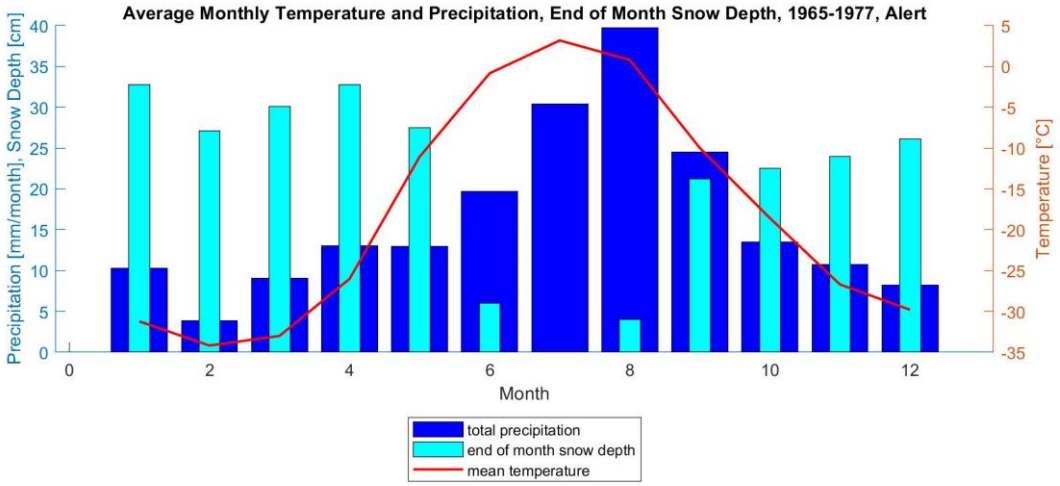

Figure Appendix 11: Climate data (total precipitation, end of month snow depth, mean temperature) used in model, Alert (Canada 2021a)

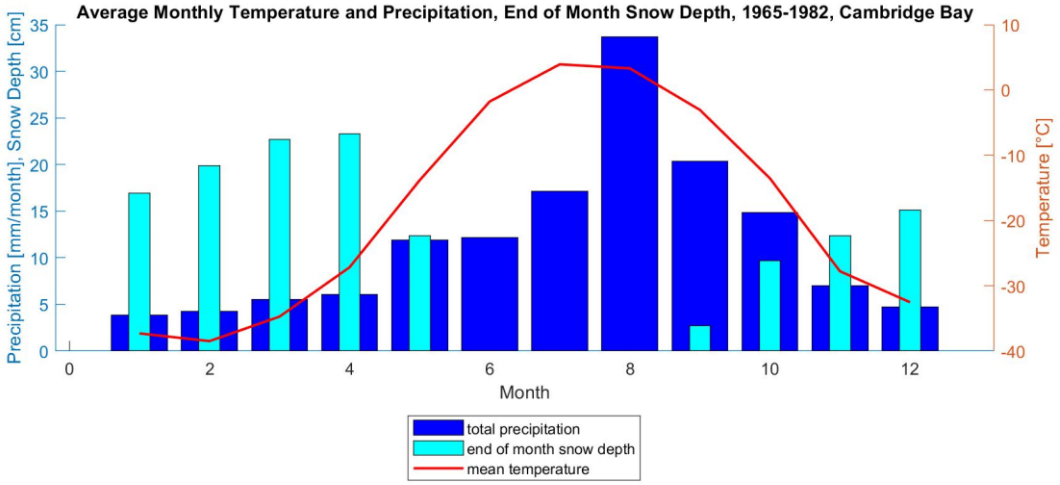

Figure Appendix 12: Climate data (total precipitation, end of month snow depth, mean temperature) used in model, Cambridge Bay (Canada 2021a)

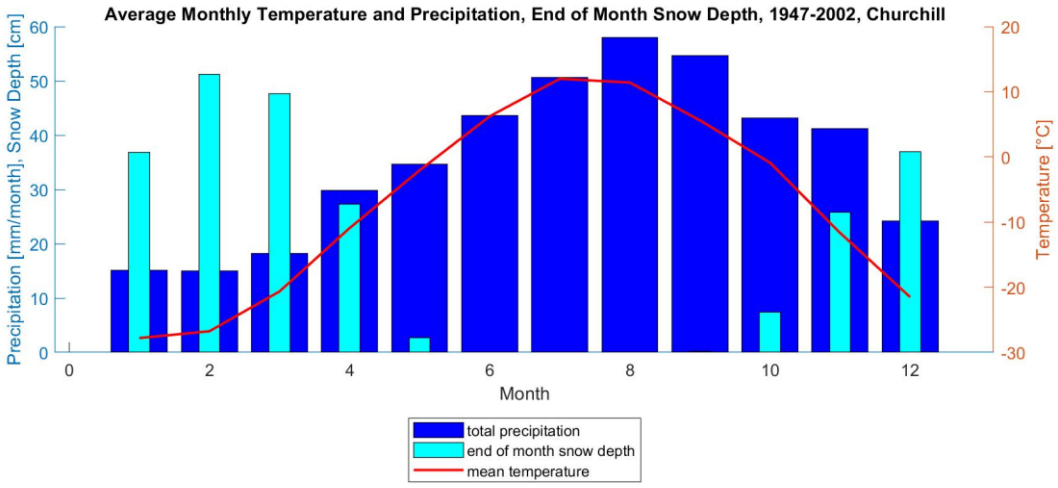

Figure Appendix 13: Climate data (total precipitation, end of month snow depth, mean temperature) used in model, Churchill (Canada 2021a)

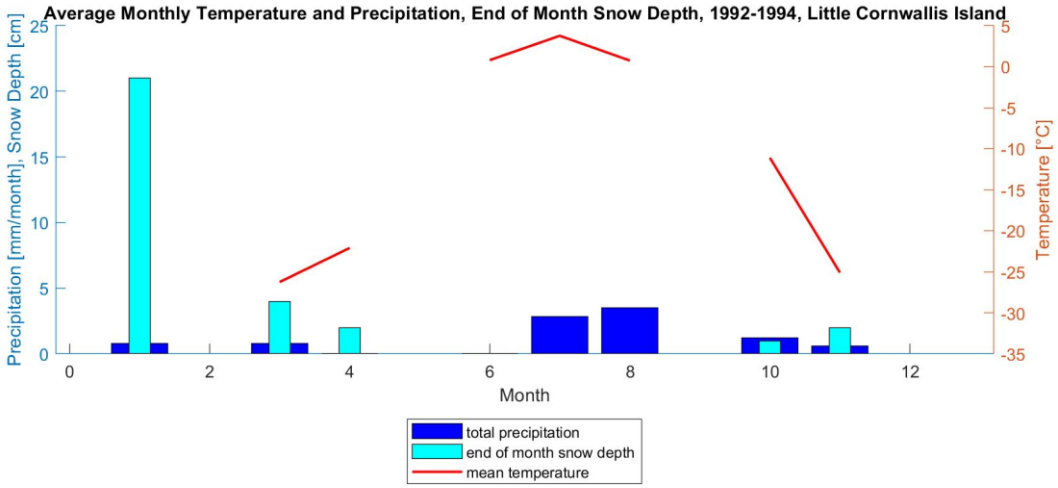

Figure Appendix 14: Climate data (total precipitation, end of month snow depth, mean temperature) used in model, Little Cornwallis Island (Canada 2021a)

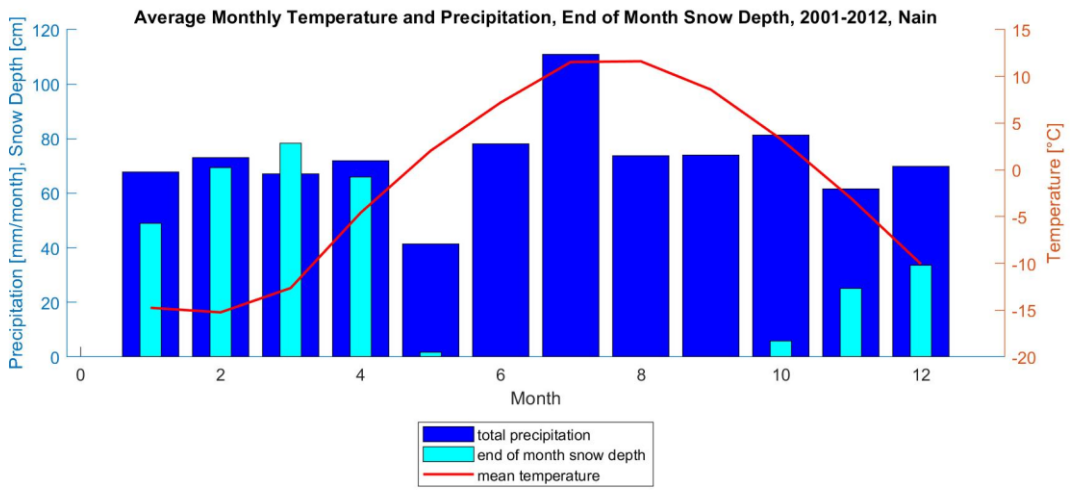

Figure Appendix 15: Climate data (total precipitation, end of month snow depth, mean temperature) used in model, Nain (Canada 2021a)

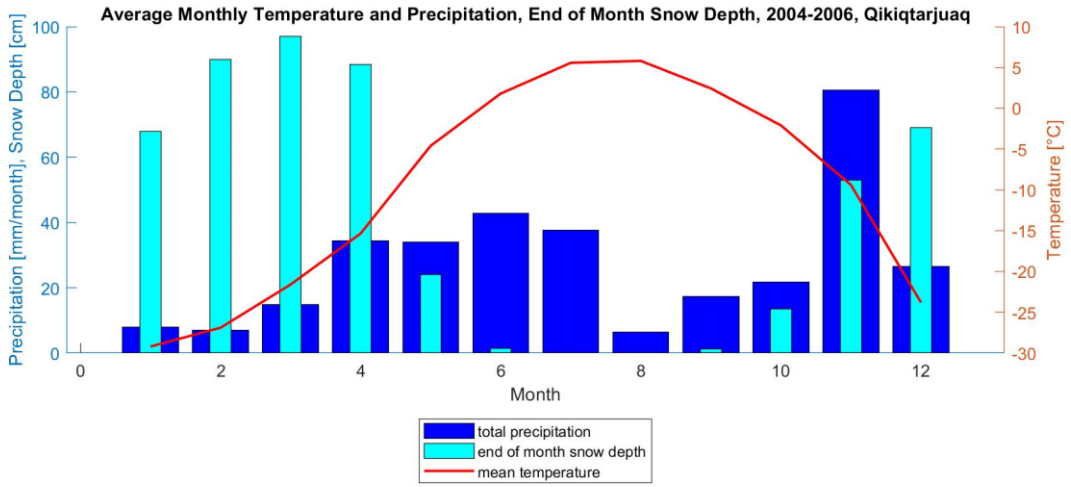

Figure Appendix 16: Climate data (total precipitation, end of month snow depth, mean temperature) used in model, Qikiqtarjuaq (Canada 2021a)

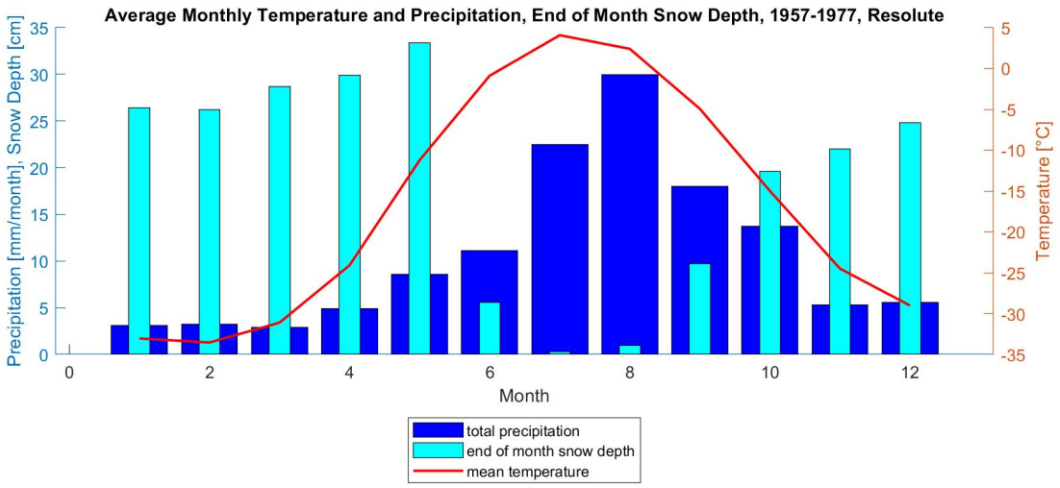

Figure Appendix 17: Climate data (total precipitation, end of month snow depth, mean temperature) used in model, Resolute (Canada 2021a)

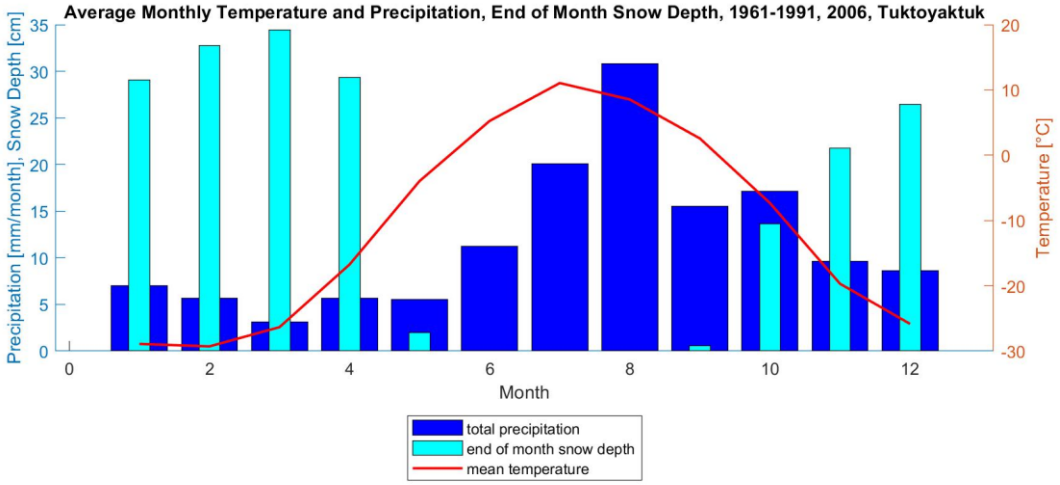

Figure Appendix 18: Climate data (total precipitation, end of month snow depth, mean temperature) used in model, Tuktoyaktuk (Canada 2021a)

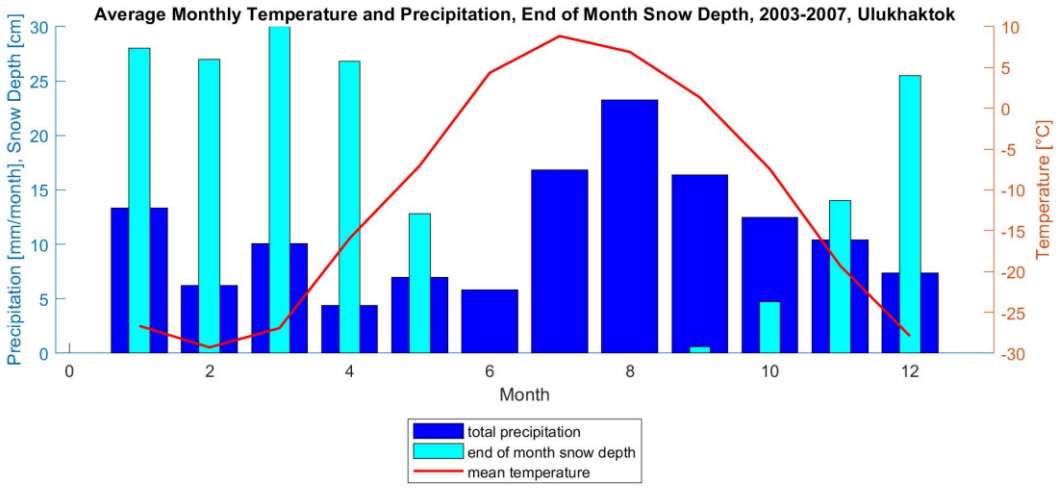

Figure Appendix 19: Climate data (total precipitation, end of month snow depth, mean temperature) used in model, Ulukhaktok (Canada 2021a)

8.6 Additional Model Outputs

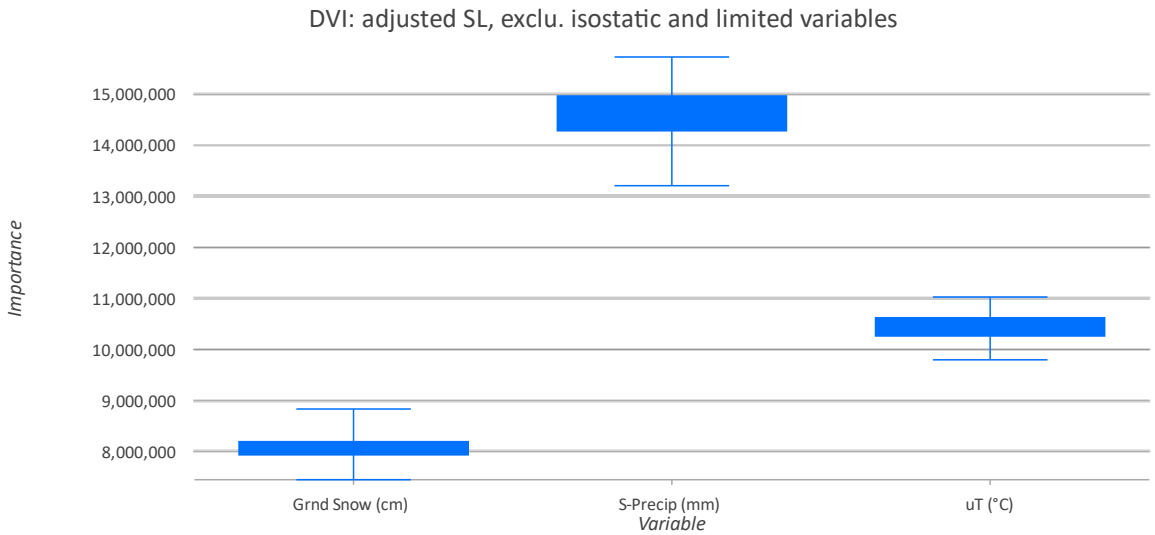

Figure Appendix 20: Distribution of Variable Importance graph for model run with adjusted sea level, excluding isostatic rebound, and limited variables. Grnd Snow is the snow on the ground, Isostatic is the isostatic rebound, S-Precip is the total precipitation, and uT is the mean temperature.

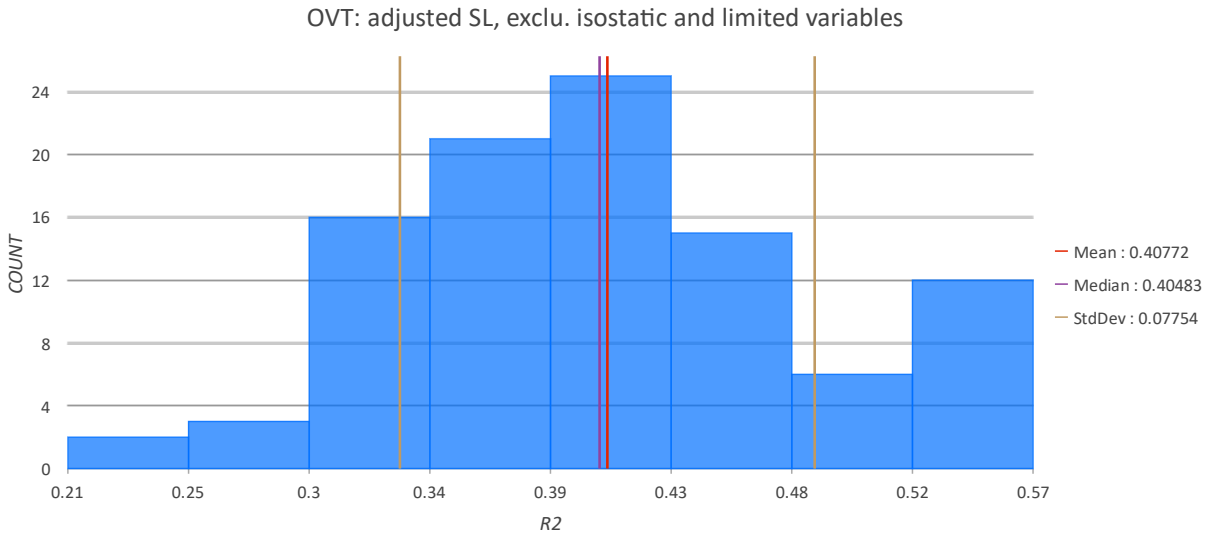

Figure Appendix 21: Output Validation Table, run on the variables from fig. Appendix 20 over 100 repetitions. This shows the R^2 values for each of the separate runs within a histogram.

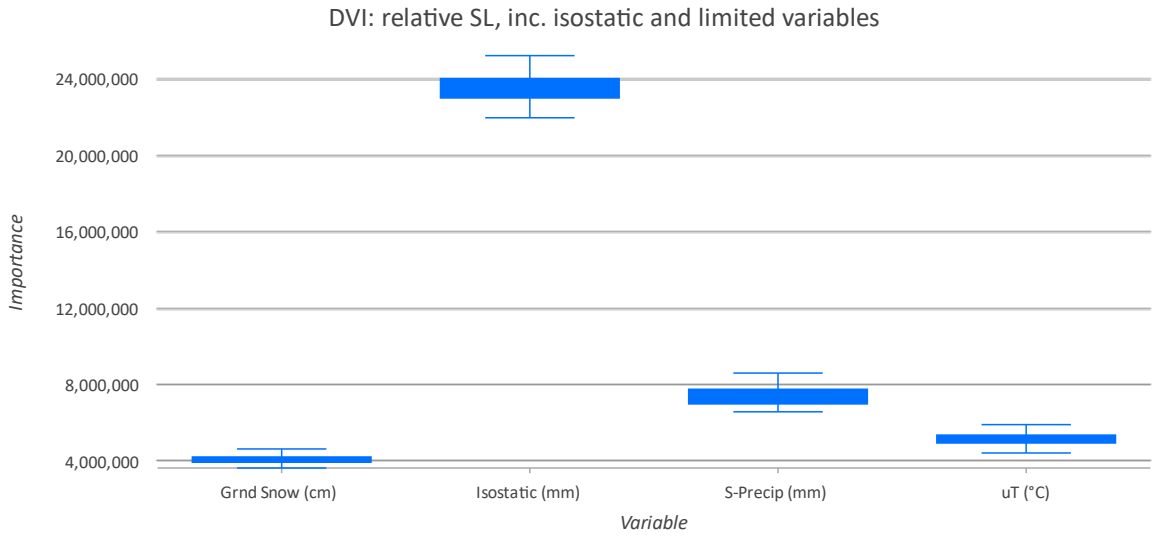

Figure Appendix 22: Distribution of Variable Importance graph for model run with relative sea level, including isostatic rebound, and limited variables. Grnd Snow is the snow on the ground, Isostatic is the isostatic rebound, S-Precip is the total precipitation, and uT is the mean temperature.

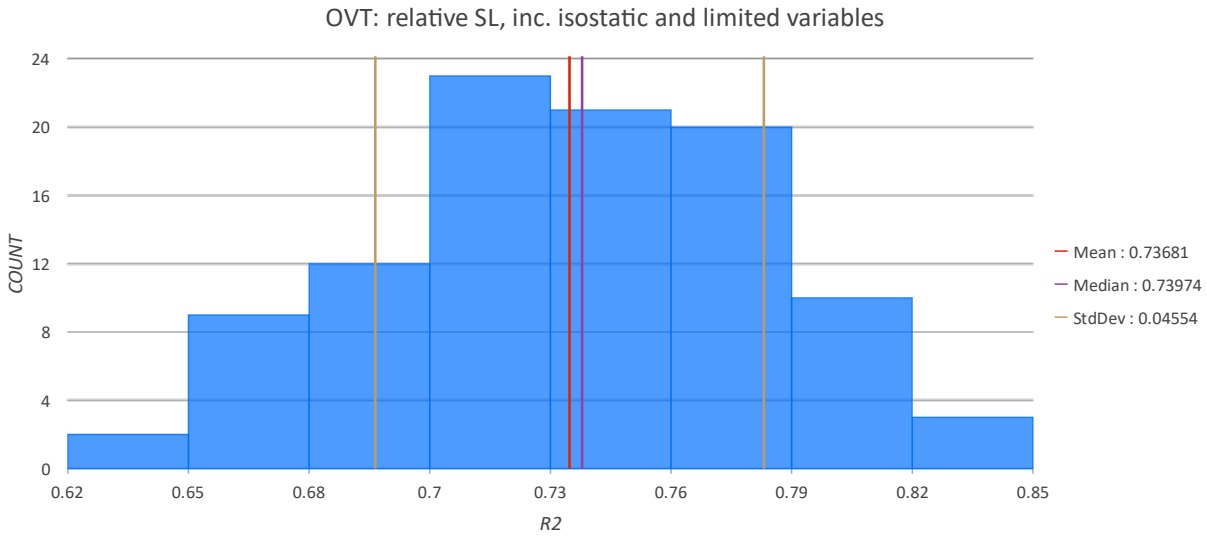

Figure Appendix 23: Output Validation Table, run on the variables from fig. Appendix 22 over 100 repetitions. This shows the R^2 values for each of the separate runs within a histogram.

Table Appendix 3: Parameter values for Forest-based regression model runs, based on 3 different years and 3 different RCP scenarios.

			Training Data Regression Diagnostics			*Validation Data Regression Diagnostics*		
Year	RCP scenario	Percentage of the variation explained	R-squared	p-value	Standard Error	R-squared	p-value	Standard Error
2035	2.6	73.2	0.921	0.000	0.007	0.733	0.000	0.038
	4.5	73.0	0.924	0.000	0.007	0.743	0.000	0.039
	8.5	73.0	0.922	0.000	0.007	0.747	0.000	0.039
2065	2.6	72.3	0.919	0.000	0.007	0.740	0.000	0.036
	4.5	72.9	0.922	0.000	0.007	0.748	0.000	0.038
	8.5	72.9	0.917	0.000	0.007	0.746	0.000	0.032
2100	2.6	72.6	0.921	0.000	0.007	0.747	0.000	0.039
	4.5	73.0	0.924	0.000	0.007	0.742	0.000	0.039
	8.5	73.1	0.924	0.000	0.007	0.740	0.000	0.042

8.7 Future Climate Data

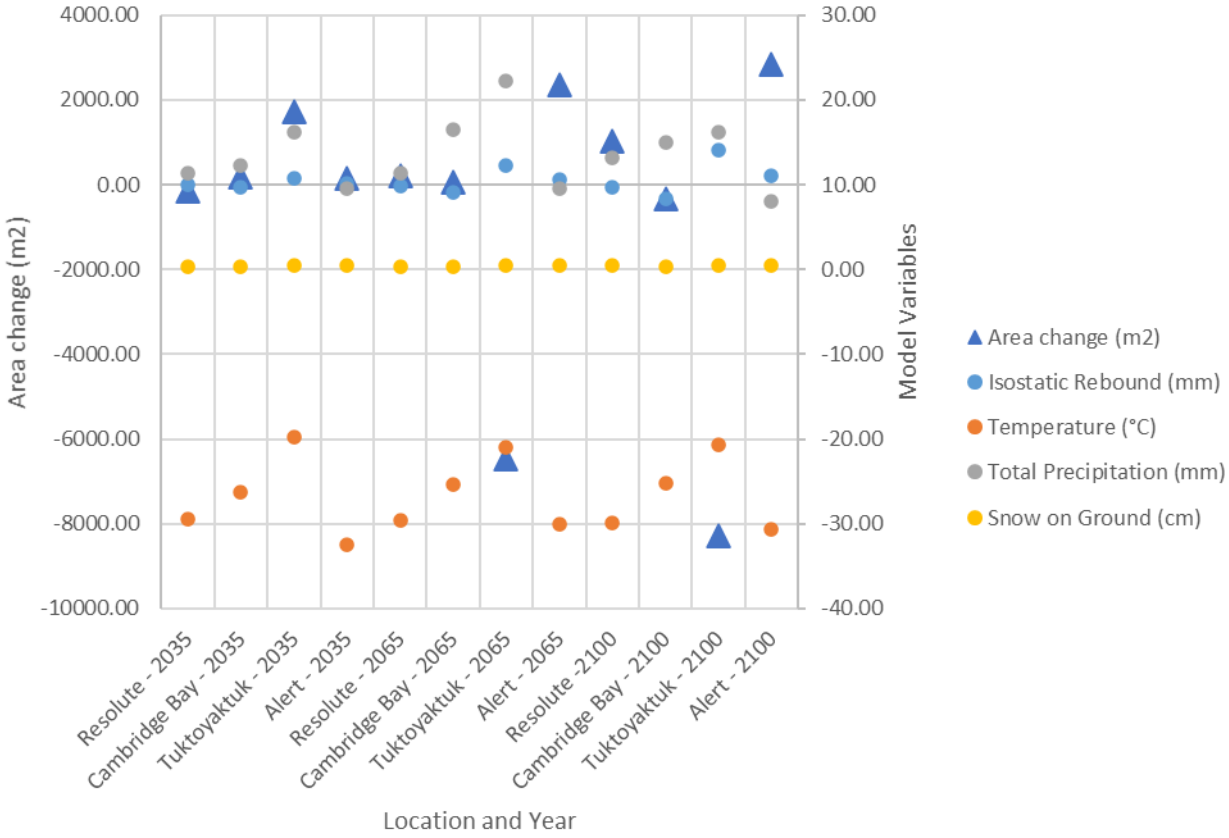

Figure Appendix 24: Area change from current coastline compared to future model data, RCP 2.6.

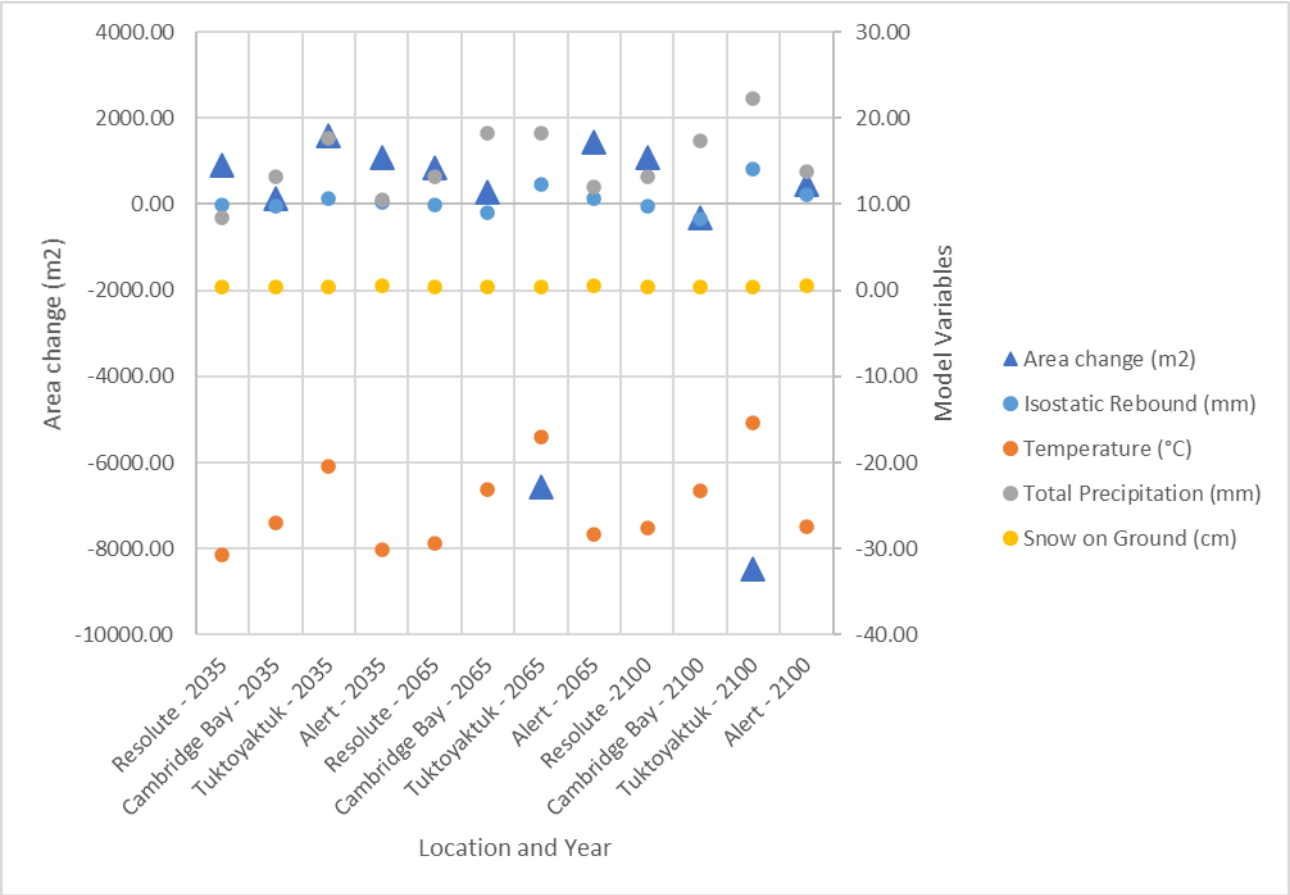

Figure Appendix 25: Area change from current coastline compared to future model data, RCP 4.5.

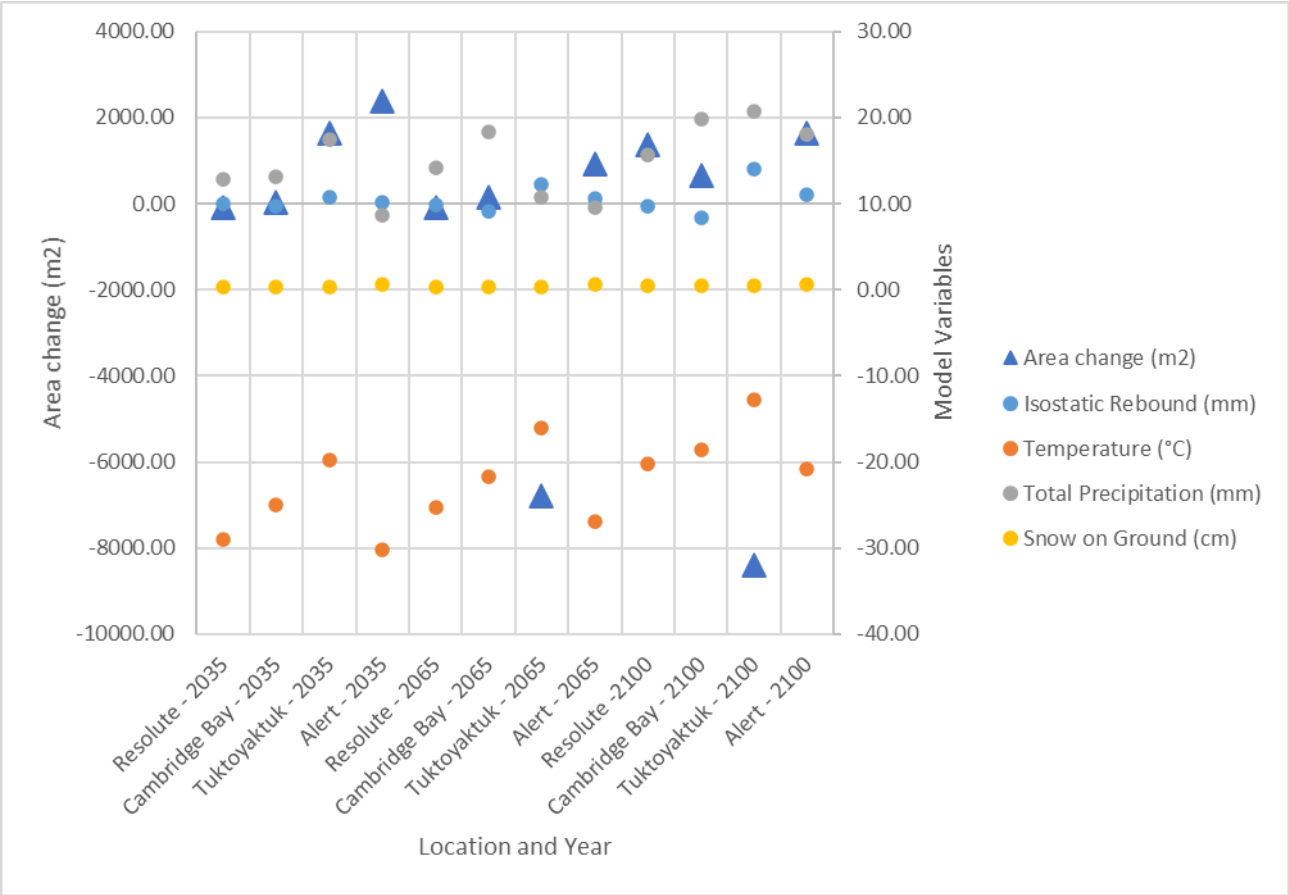

Figure Appendix 26: Area change from current coastline compared to future model data, RCP 8.5.